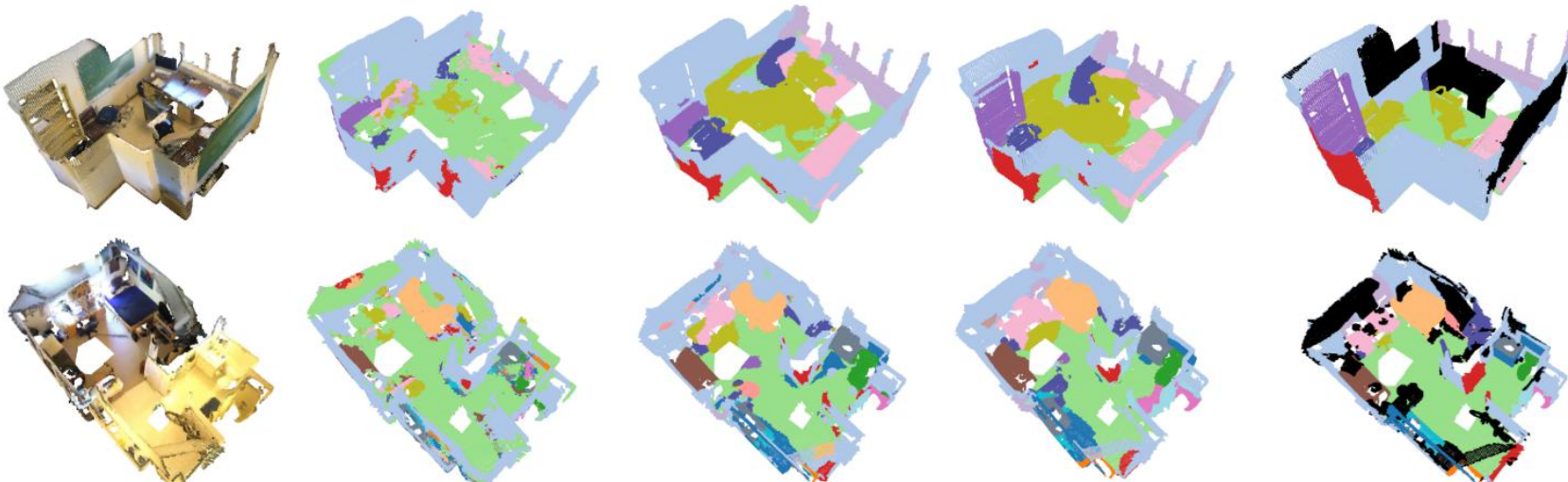
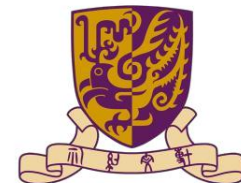


# *Deep Learning for 3D Point Cloud Analysis*



Xu Yan  
2020.8.20



香港中文大學(深圳)  
The Chinese University of Hong Kong, Shenzhen



# Paper List



香港中文大學(深圳)  
The Chinese University of Hong Kong, Shenzhen



- PointContrast: Unsupervised Pre-training for 3D Point Cloud Understanding (ECCV2020 **spotlight**)
- A Closer Look at Local Aggregation Operators in Point Cloud Analysis (ECCV2020)
- Towards Content-Independent Multi-Reference Super-Resolution: Adaptive Pattern Matching and Feature Aggregation (ECCV2020)

# PointContrast



香港中文大學(深圳)  
The Chinese University of Hong Kong, Shenzhen



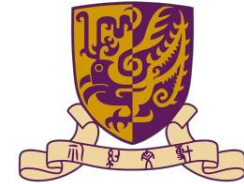
## PointContrast: Unsupervised Pre-training for 3D Point Cloud Understanding

Saining Xie<sup>1</sup>, Jiatao Gu<sup>1</sup>, Demi Guo\*, Charles R. Qi\*,  
Leonidas Guibas<sup>2\*</sup>, and Or Litany<sup>2\*</sup>

<sup>1</sup> Facebook AI Research

<sup>2</sup> Stanford University

# PointContrast



香港中文大學(深圳)  
The Chinese University of Hong Kong, Shenzhen



All existing representation learning schemes are tested either on single objects or low-level tasks (e.g. registration). This status quo can be attributed to multiple reasons:

- 1) Lack of large-scale and high-quality **data**: compared to 2D images, 3D data is harder to collect, more expensive to label, and the variety of sensing devices may introduce drastic domain gaps;
- 2) Lack of unified **backbone** architectures: in contrast to 2D vision where architectures such as ResNets have proven successful as backbone networks for pre-training and fine-tuning, point cloud network architecture designs are still evolving;
- 3) Lack of a comprehensive set of datasets and high-level tasks for **evaluation**.

# PointContrast



香港中文大學(深圳)  
The Chinese University of Hong Kong, Shenzhen

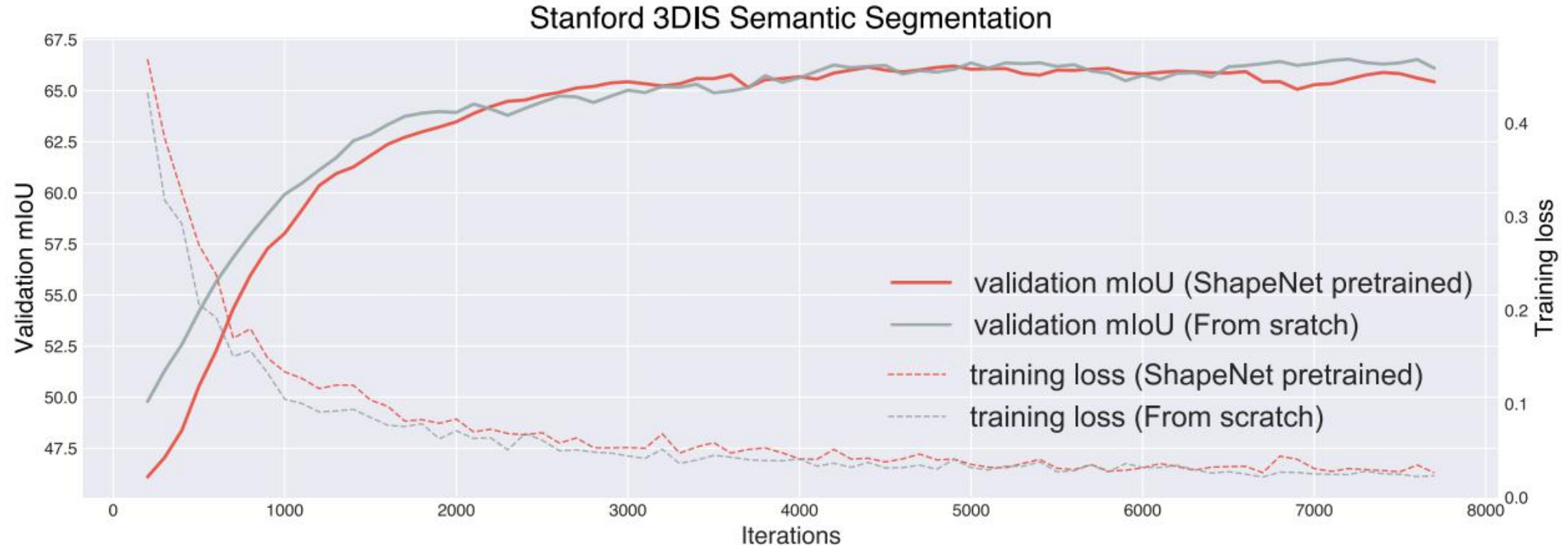
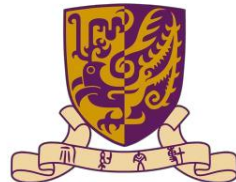


Fig. 1: Training from scratch *vs.* fine-tuning with ShapeNet pre-trained weights.

# PointContrast



香港中文大學(深圳)  
The Chinese University of Hong Kong, Shenzhen

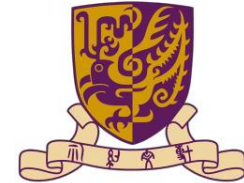


| PointContrast: Downstream Tasks for Fine-tuning |                  |                                 |                     |                |              |        |
|---|------------------|---------------------------------|---------------------|----------------|--------------|--------|
| Datasets  | Real /<br>Synth. | Complexity                      | Env.                | Task           | Rel.<br>gain |        |
| S3DIS   | Real             | Entire floor,<br>office         | Indoor              | Segmentation   | (+2.7%)      | mIoU   |
| SUN RGB-D                                       | Real             | Medium-sized<br>cluttered rooms | Indoor              | Detection      | (+3.1%)      | mAP0.5 |
| ScanNetV2                                       | Real             | Large rooms                     | Indoor              | Segmentation   | (+1.9%)      | mIoU   |
|   |                  | Large rooms                     | Indoor &<br>outdoor | Detection      | (+2.6%)      | mAP0.5 |
| ShapeNet  | Synth.           | Single objects                  |                     | Classification | (+4.0%)      | Acc.*  |
| ShapeNetPart                                    | Synth.           | Object parts                    | Indoor &<br>outdoor | Segmentation   | (+2.2%)      | mIoU*  |
| Synthia 4D                                      | Synth.           | Street scenes,<br>driving envs. | Outdoor             | Segmentation   | (+3.3%)      | mIoU   |

Table 1: **Summary of downstream fine-tuning tasks.** Compared to the baseline learning paradigm of training from scratch, which is dominant in 3D deep learning, our unsupervised pre-training method PointContrast boosts the performance across the board when finetuning on a diverse set of high-level 3D understanding tasks.

\* indicates results trained using only 1% of the training data.

# PointContrast



香港中文大學(深圳)  
The Chinese University of Hong Kong, Shenzhen



- **Domain gap between source and target data:** Objects in ShapeNet are synthetic, normalized in scale, aligned in pose, and lack scene context. This makes pre-training and fine-tuning data distributions drastically different.
- **Point-level representation matters:** In 3D deep learning, the local geometric features, *e.g.* those encoded by a point and its neighbors, have proven to be discriminative and critical for 3D tasks [47, 48]. Directly training on *object instances* to obtain a global representation might be insufficient.

# PointContrast



香港中文大學(深圳)  
The Chinese University of Hong Kong, Shenzhen



---

## Algorithm 1 General Framework of PointContrast

---

**Input:** Backbone architecture NN; Dataset  $X = \{\mathbf{x}_i \in \mathbb{R}^{N \times 3}\}$ ; Point feature dimension  $D$ ;

**Output:** Pre-trained weights for NN.

**for** each point cloud  $\mathbf{x}$  in  $X$  **do**

- From  $\mathbf{x}$ , generate two views  $\mathbf{x}^1$  and  $\mathbf{x}^2$ .
- Compute correspondence mapping (matches)  $M$  between points in  $\mathbf{x}^1$  and  $\mathbf{x}^2$ .
- Sample two transformations  $\mathbf{T}_1$  and  $\mathbf{T}_2$ .
- Compute point features  $\mathbf{f}^1, \mathbf{f}^2 \in \mathbb{R}^{N \times D}$  by  
 $\mathbf{f}^1 = \text{NN}(\mathbf{T}_1(\mathbf{x}^1))$  and  $\mathbf{f}^2 = \text{NN}(\mathbf{T}_2(\mathbf{x}^2))$ .
- Backprop. to update NN with contrastive loss  $\mathcal{L}_c(\mathbf{f}^1, \mathbf{f}^2)$  on the matched points.

**end**

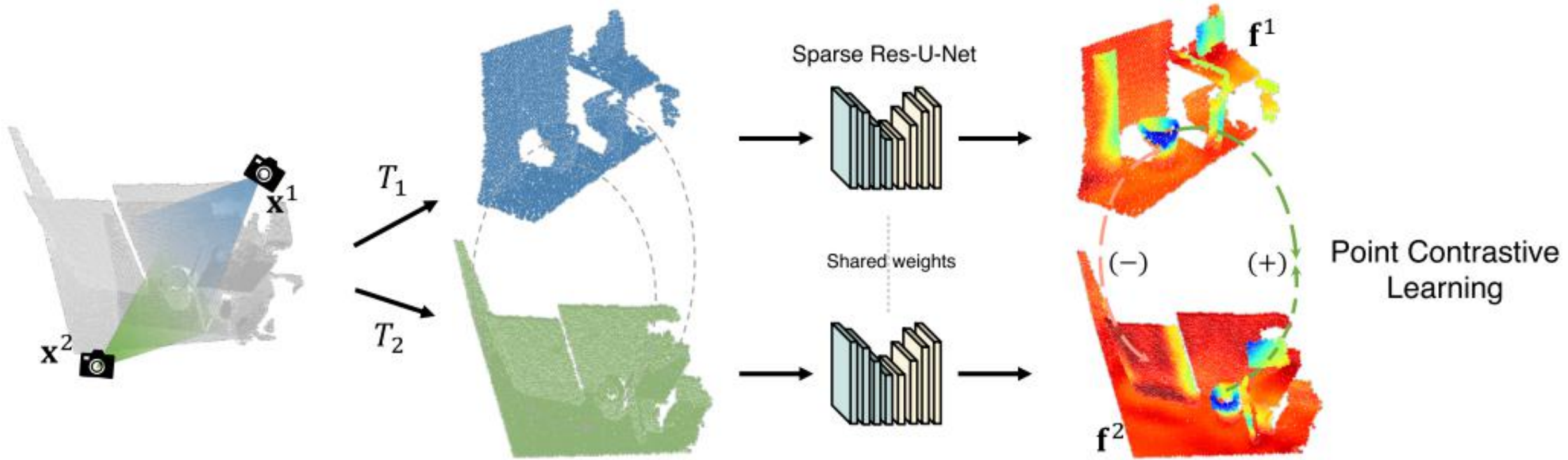
---

# PointContrast



香港中文大學(深圳)  
The Chinese University of Hong Kong, Shenzhen

Fig. 2: PointContrast: Pretext task for 3D pre-training.



# PointContrast



香港中文大學(深圳)  
The Chinese University of Hong Kong, Shenzhen

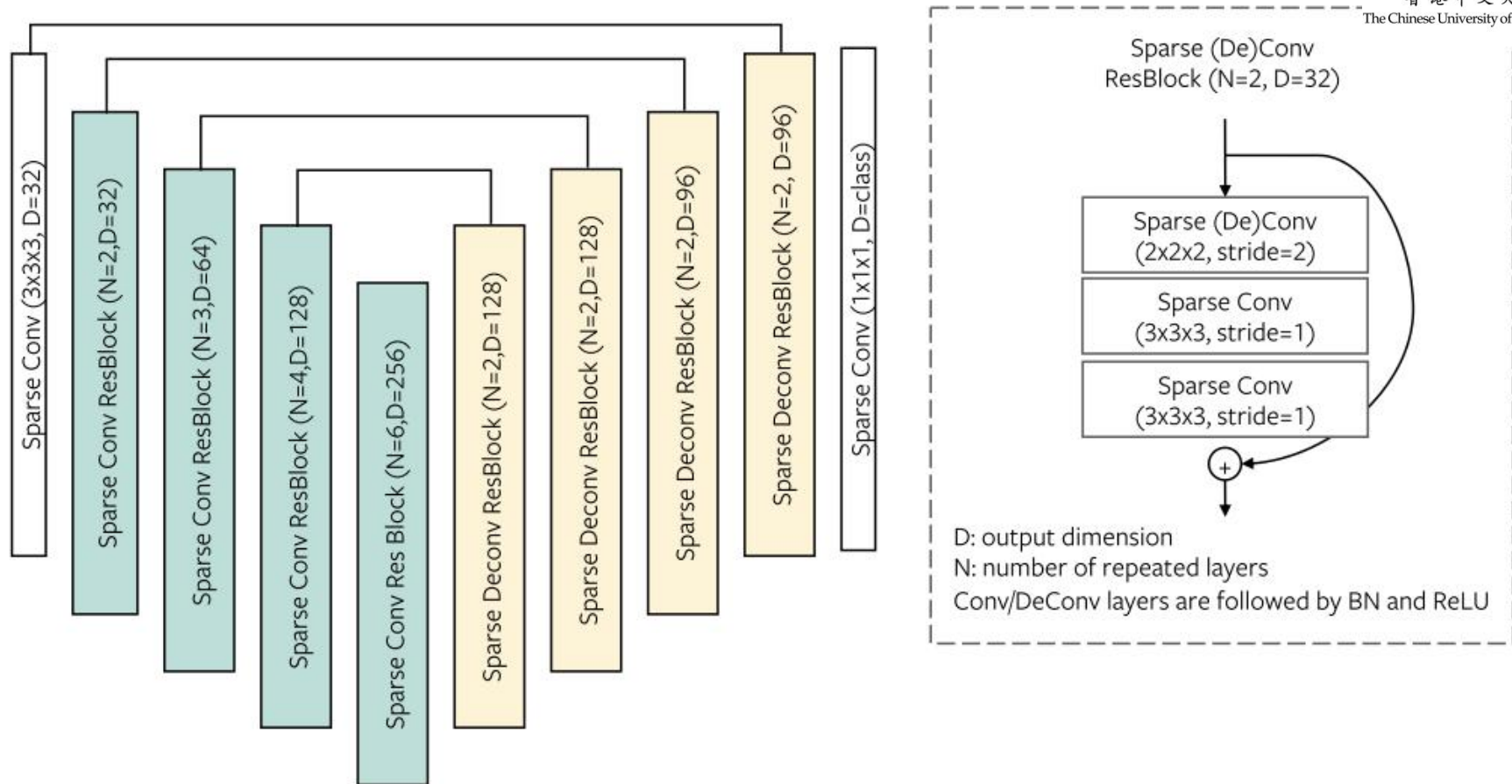


Fig. 3: SR-UNet architecture we used as a shared backbone network for pre-training and fine-tuning tasks. For segmentation and detection tasks, both the encoder and decoder weights are fine-tuned; for classification downstream tasks, only the encoder network is kept and fine-tuned.

# PointContrast



香港中文大學(深圳)  
The Chinese University of Hong Kong, Shenzhen



## Hardest-Contrastive Loss

$$\mathcal{L}_c = \sum_{(i,j) \in \mathcal{P}} \left\{ [d(\mathbf{f}_i, \mathbf{f}_j) - m_p]_+^2 / |\mathcal{P}| + 0.5[m_n - \min_{k \in \mathcal{N}} d(\mathbf{f}_i, \mathbf{f}_k)]_+^2 / |\mathcal{N}_i| + 0.5[m_n - \min_{k \in \mathcal{N}} d(\mathbf{f}_j, \mathbf{f}_k)]_+^2 / |\mathcal{N}_j| \right\}$$

Here P is a set of matched (**positive**) pairs of points and N is a randomly sampled set of non-matched (**negative**) points which is used for the hardest negative mining, where the hardest sample is defined as the closest point in the L2 normalized feature space to a positive pair.  $[x]_+$  denotes function  $\max(0, x)$ .  $m_p = 0.1$  and  $m_n = 1.4$  are margins for positive and negative pairs.

## PointInfoNCE Loss

$$\mathcal{L}_c = - \sum_{(i,j) \in \mathcal{P}} \log \frac{\exp(\mathbf{f}_i \cdot \mathbf{f}_j / \tau)}{\sum_{(\cdot,k) \in \mathcal{P}} \exp(\mathbf{f}_i \cdot \mathbf{f}_k / \tau)}$$

# PointContrast



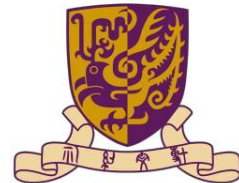
香港中文大學(深圳)  
The Chinese University of Hong Kong, Shenzhen



| evaluating on all 55 classes        | 1% data            | 10% data           | 100% data          |
|-------------------------------------|--------------------|--------------------|--------------------|
| Trained from scratch                | 62.2               | 77.9               | 85.1               |
| PointContrast (Hardest-Contrastive) | <b>66.2</b> (+4.0) | <b>79.0</b> (+1.1) | <b>85.7</b> (+0.6) |
| PointContrast (PointInfoNCE)        | <b>65.8</b> (+3.6) | <b>78.8</b> (+0.9) | <b>85.7</b> (+0.6) |
| using 100% training data            | 10 tail classes    | 30 tail classes    | all 55 classes     |
| Train from scratch                  | 65.0               | 70.9               | 85.1               |
| PointContrast (Hardest-Contrastive) | <b>70.9</b> (+5.9) | <b>72.9</b> (+2.0) | <b>85.7</b> (+0.6) |
| PointContrast (PointInfoNCE)        | <b>67.8</b> (+2.8) | <b>72.0</b> (+1.1) | <b>85.7</b> (+0.6) |

Table 2: **ShapeNet classification.** Top: classification accuracy with limited labeled training data for finetuning. Bottom: classification accuracy on the least represented classes in the data (tail-classes). In all cases, PointContrast boosts performance. Relative improvement increases with scarcer training data and on less frequent classes.

# PointContrast



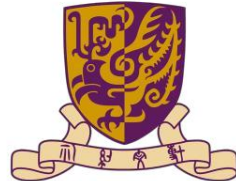
香港中文大學(深圳)  
The Chinese University of Hong Kong, Shenzhen



| methods                             | IoU (1% data)      | IoU (5% data)      | IoU (100% data)    |
|-------------------------------------|--------------------|--------------------|--------------------|
| SO-Net[36]                          | 64.0               | 69.0               | -                  |
| PointCapsNet[85]                    | 67.0               | 70.0               | -                  |
| Multitask Unsupervised[22]          | 68.2               | 77.7               | -                  |
| Train from scratch                  | 71.8               | 79.3               | 84.7               |
| PointContrast (Hardest-Contrastive) | <b>74.0</b> (+2.2) | <b>79.9</b> (+0.6) | <b>85.1</b> (+0.4) |
| PointContrast (PointInfoNCE)        | <b>73.1</b> (+1.3) | <b>79.9</b> (+0.6) | <b>85.1</b> (+0.4) |

Table 3: **ShapeNet part segmentation.** Replacing the backbone architecture with SR-UNet already boosts performance. PointContrast pre-training further adds a significant gain, and outshines where labels are most limited.

# PointContrast



香港中文大學(深圳)  
The Chinese University of Hong Kong, Shenzhen



| methods                             | mIoU               | mAcc               |
|-------------------------------------|--------------------|--------------------|
| PointNet [47]                       | 41.1               | 49.0               |
| PointCNN [37]                       | 57.3               | 63.9               |
| MinkowskiNet32 [9]                  | 65.4               | 71.7               |
| Train from scratch                  | 68.2               | 75.5               |
| PointContrast (Hardest-Contrastive) | <b>70.9</b> (+2.7) | <b>77.0</b> (+1.5) |
| PointContrast (PointInfoNCE)        | 70.3 (+2.1)        | 76.9 (+1.4)        |

Table 4: **Stanford Area 5 Test (Fold 1) (S3DIS)**. Replacing the backbone network with SR-UNet improves upon prior art. Using PointContrast adds further significant boost with a mild preference for Hardest-contrastive over the PointInfoNCE objective. See Appendix for more methods in comparison.

# PointContrast



香港中文大學(深圳)  
The Chinese University of Hong Kong, Shenzhen



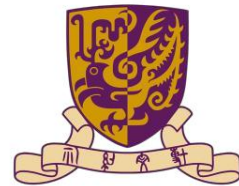
| methods                            | input      | mAP@0.5            | mAP@0.25           |
|------------------------------------|------------|--------------------|--------------------|
| VoteNet [45]                       | Geo        | -                  | 57.0               |
| VoteNet [45]                       | Geo+Height | 32.9               | 57.7               |
| Train from scratch                 | Geo        | 31.7               | 55.6               |
| PointContrast(Hardest-Contrastive) | Geo        | 34.5 (+2.8)        | <b>57.5</b> (+1.9) |
| PointContrast(PointInfoNCE)        | Geo        | <b>34.8</b> (+3.1) | <b>57.5</b> (+1.9) |

Table 5: **SUN RGB-D detection results.** PointContrast demonstrates a substantial boost compared to training from scratch. We observe a larger improvement in localization as manifested by the  $\Delta$ mAP being larger for @0.5 than @0.25.

| methods                             | mIoU               | mAcc               |
|-------------------------------------|--------------------|--------------------|
| MinkowskiNet32 [9]                  | 78.7               | 91.5               |
| Train from scratch                  | 79.8               | 91.5               |
| PointContrast (Hardest-Contrastive) | 82.6 (+2.8)        | <b>93.7</b> (+2.2) |
| PointContrast (PointInfoNCE)        | <b>83.1</b> (+3.3) | <b>93.7</b> (+2.2) |

Table 6: **Segmentation results on the 4D Synthia test set.** All networks here are SR-UNet with 3D kernels, trained on individual 3D frames without temporal modeling.

# PointContrast



| methods                            | mIoU               | mAcc               |
|------------------------------------|--------------------|--------------------|
| Train from scratch                 | 72.2               | 80.7               |
| PointContrast(Hardest-Contrastive) | 73.3 (+1.1)        | 81.0 (+0.3)        |
| PointContrast(PointInfoNCE)        | <b>74.1 (+1.9)</b> | <b>81.6 (+0.9)</b> |

Table 7: **Segmentation results on ScanNet validation set.** PointContrast boosts performance on the “in-domain” transfer task where the pre-training and fine-tuning datasets come from a common source, showing the usefulness of pre-training even when labels are available.

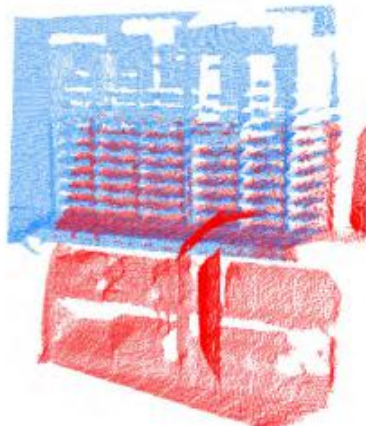
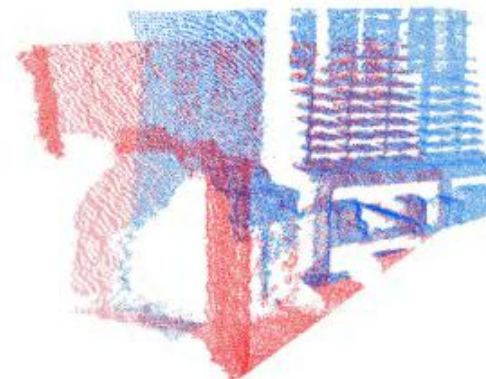
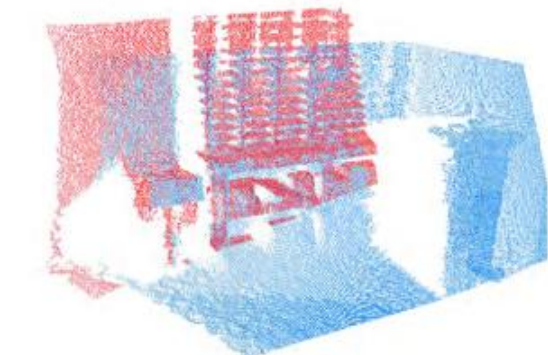
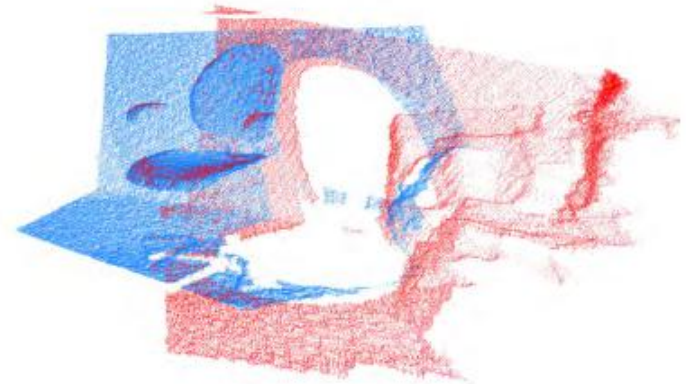
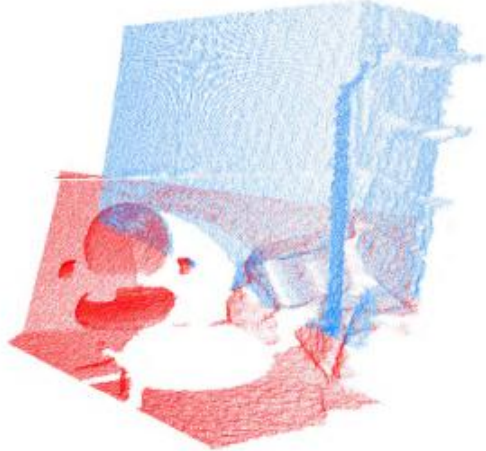
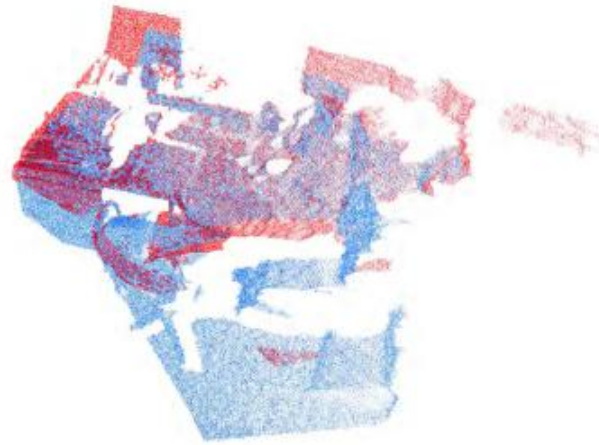
| methods                            | input             | mAP@0.5            | mAP@0.25           |
|------------------------------------|-------------------|--------------------|--------------------|
| DSS [58, 29]                       | Geo+RGB           | 6.8                | 15.2               |
| 3D-SIS [29]                        | Geo+RGB (5 Views) | 22.5               | 40.2               |
| VoteNet [45]                       | Geo+Height        | 33.5               | 58.6               |
| Train from scratch                 | Geo               | 35.4               | 56.7               |
| PointContrast(Hardest-Contrastive) | Geo               | 37.3 (+1.9)        | <b>59.2 (+2.5)</b> |
| PointContrast(PointInfoNCE)        | Geo               | <b>38.0 (+2.6)</b> | 58.5 (+1.8)        |

Table 8: **3D object detection results on ScanNet validation set.** Similarly to in-domain *segmentation* task, here as well PointContrast boost performance on *detection*, setting a new best result over prior art. See Appendix for more methods in comparison.

# PointContrast



香港中文大學(深圳)  
The Chinese University of Hong Kong, Shenzhen





## A Closer Look at Local Aggregation Operators in Point Cloud Analysis

Ze Liu<sup>1,2\*</sup>, Han Hu<sup>2\*</sup>, Yue Cao<sup>2</sup>, Zheng Zhang<sup>2</sup>, and Xin Tong<sup>2</sup>

<sup>1</sup> University of Science and Technology of China

liuze@mail.ustc.edu.cn

<sup>2</sup> Microsoft Research Asia

{hanhu,yuecao,zhez,xtong}@microsoft.com

<https://github.com/zeliu98/CloserLook3D>

# Closer Look



香港中文大學(深圳)  
The Chinese University of Hong Kong, Shenzhen



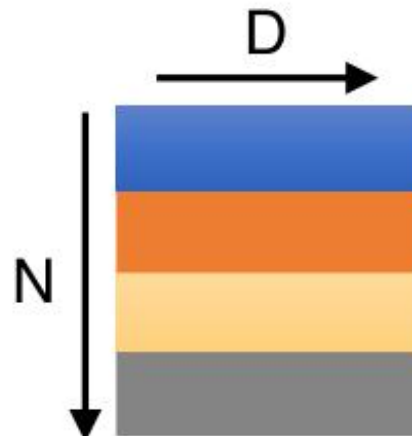
- The investigation reveals that despite the different designs of these operators, all of these operators **make surprisingly similar contributions** to the network performance under the same network input and feature numbers and result in the state-of-the-art accuracy on standard benchmarks.
- Propose a simple local aggregation operator without learnable weights, named **Position Pooling (PosPool)**, which performs similarly or slightly better than existing sophisticated operators.

# Closer Look

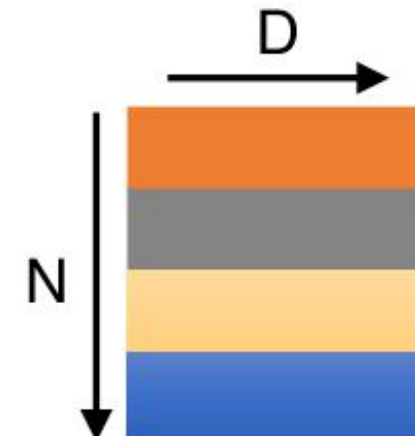
The model has respect properties of point clouds

## Permutation Invariance

- Point cloud is a set of unordered points



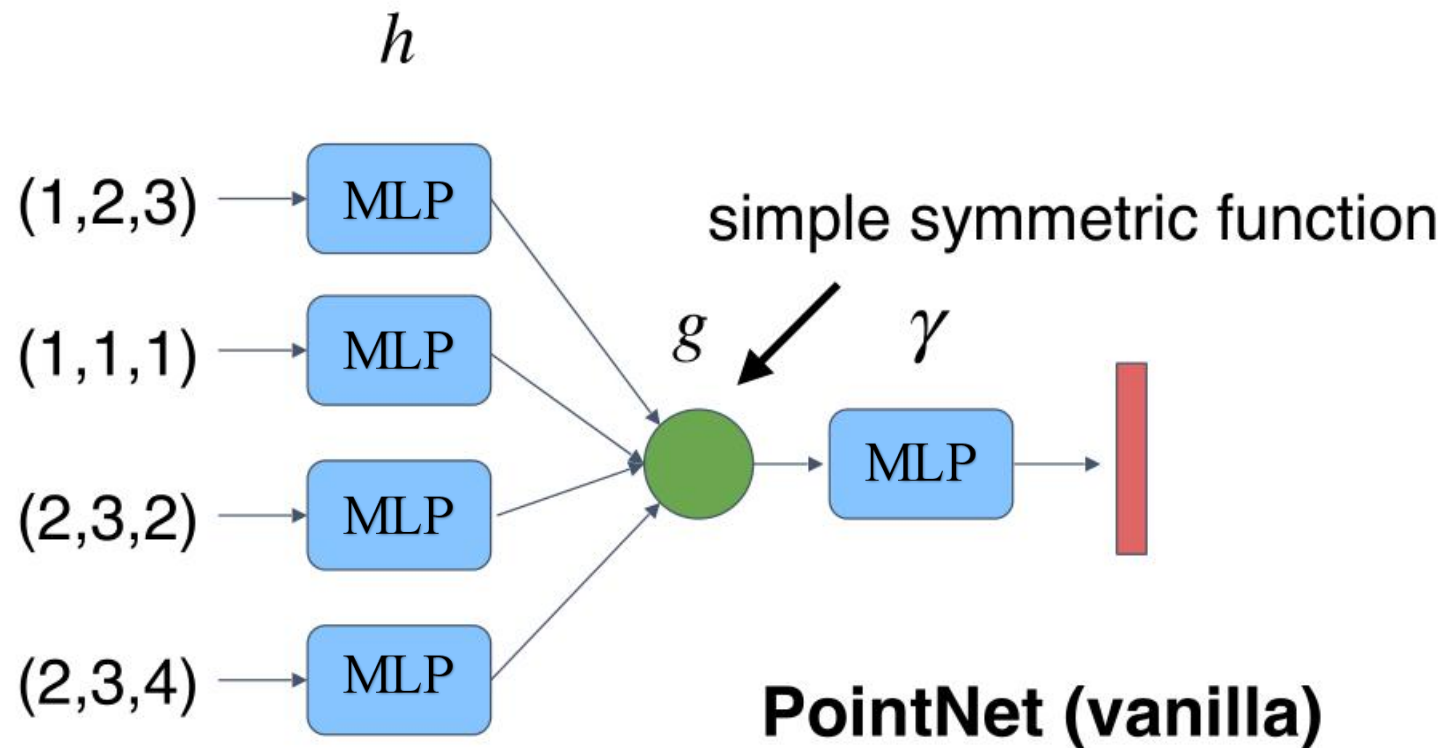
represents the same **set** as



2D array representation

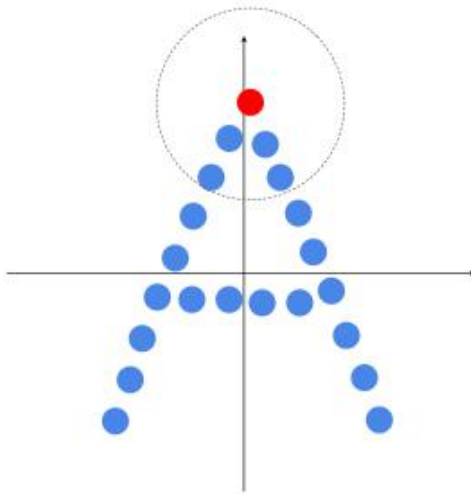
# Closer Look

## Symmetric function

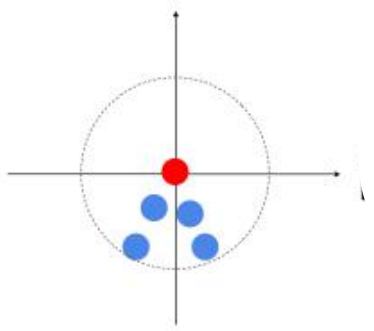


**Observe:**  $f(x_1, x_2, \dots, x_n) = \gamma \circ g(h(x_1), \dots, h(x_n))$  is symmetric if  $g$  is symmetric

# Closer Look

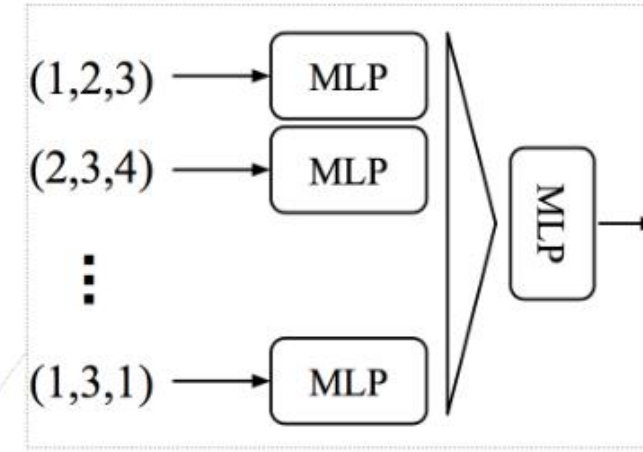
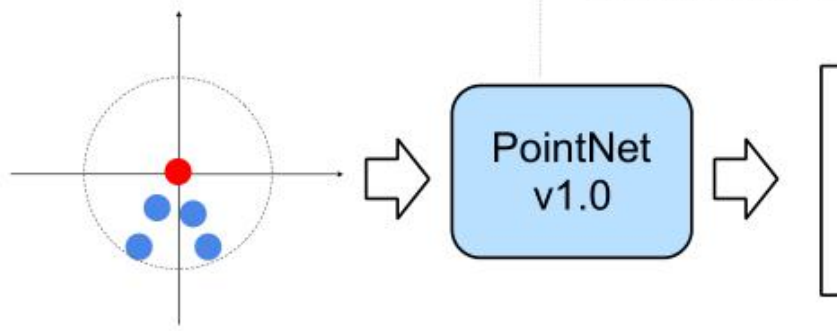
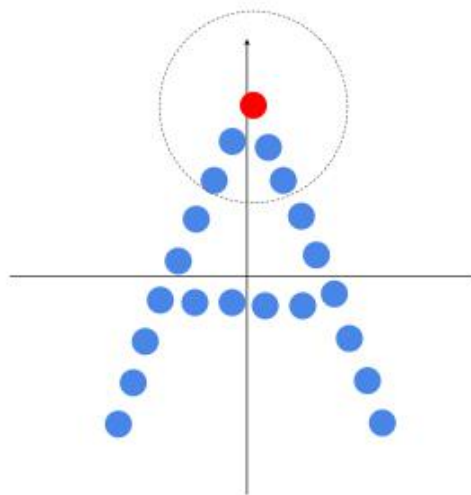


$N$  points in  $(x, y)$



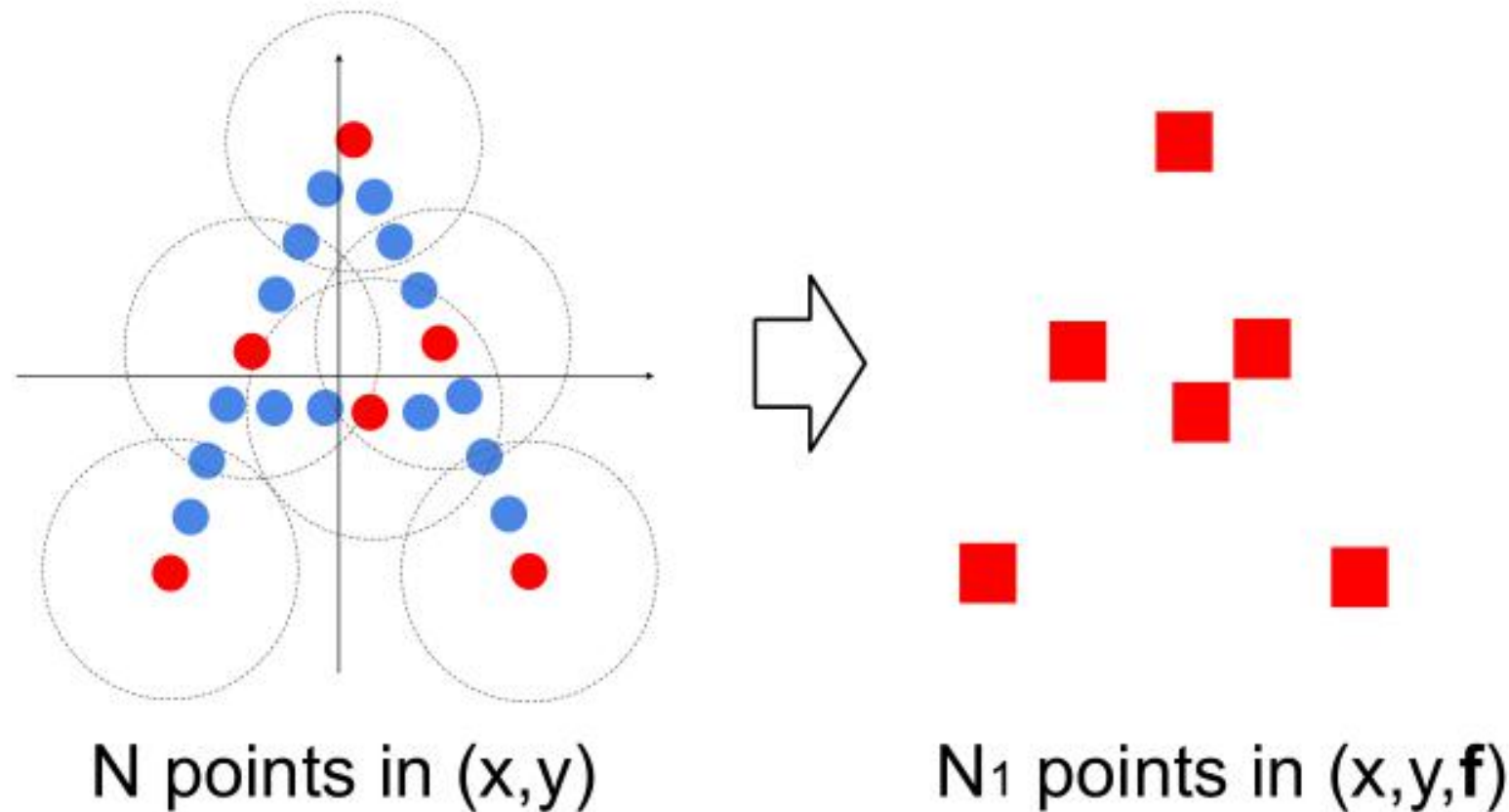
$k$  local points in  $(x', y')$

# Closer Look

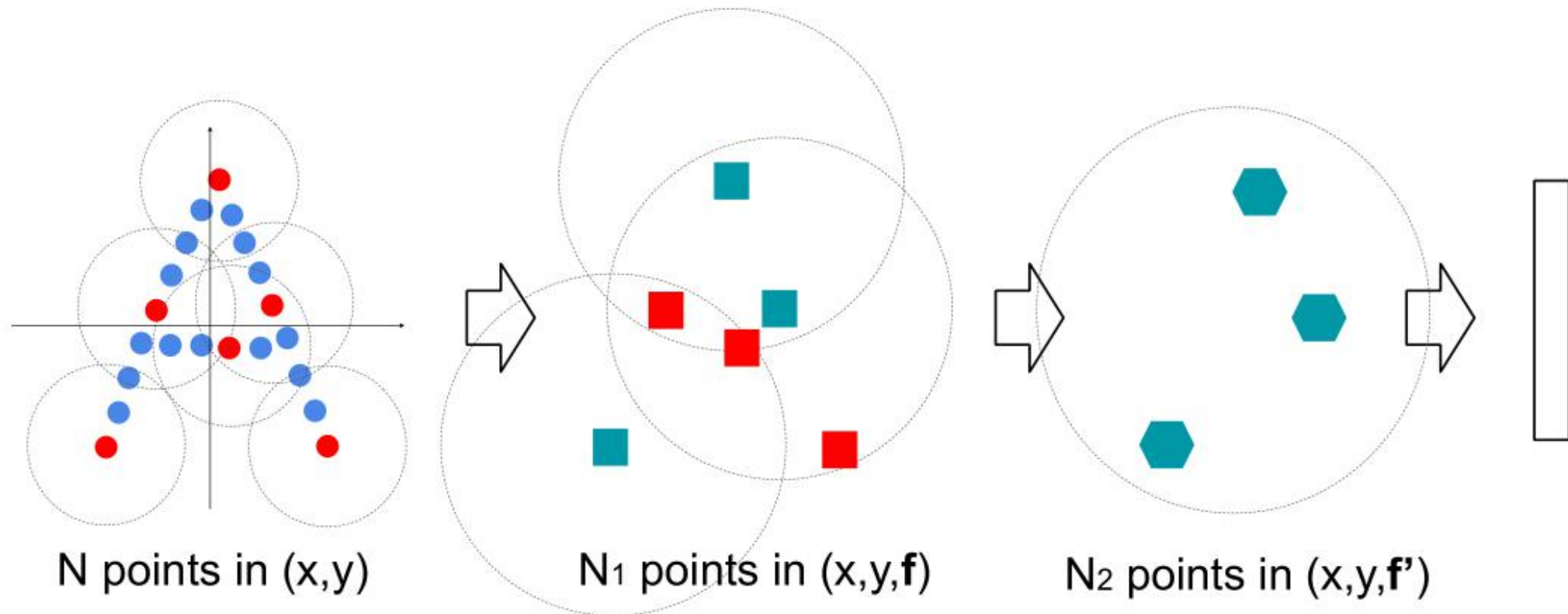


feature vector (mark as ■)  
for local point cloud

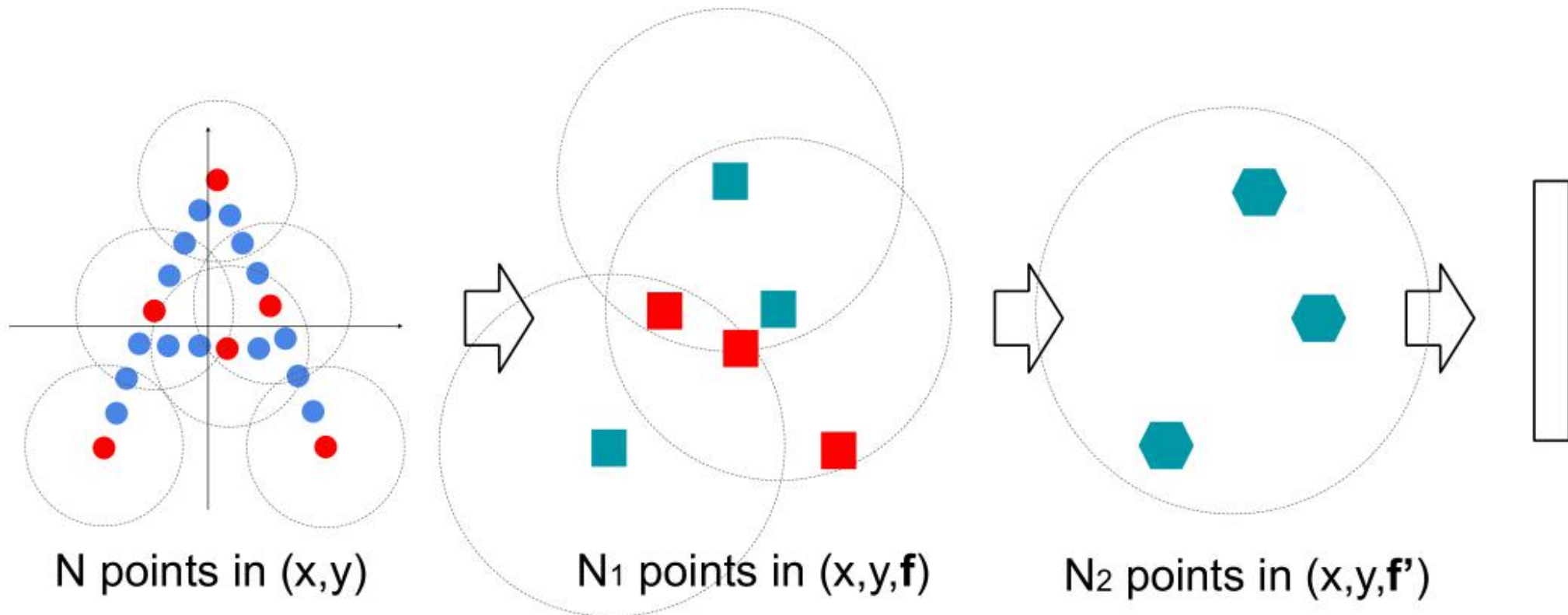
# Closer Look



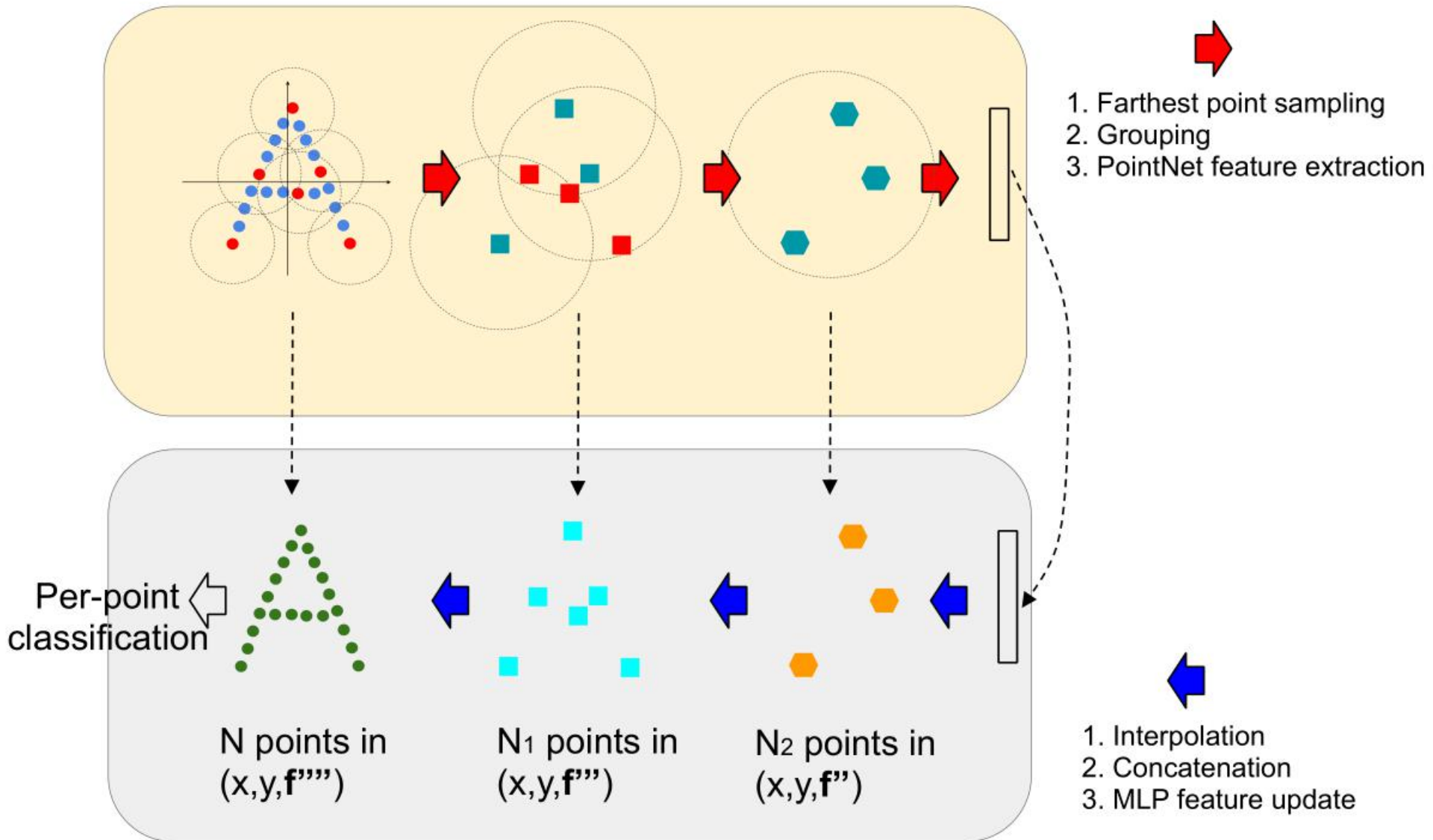
# Closer Look



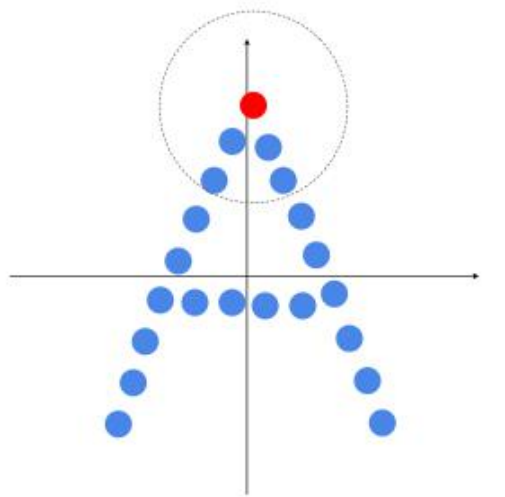
# Closer Look



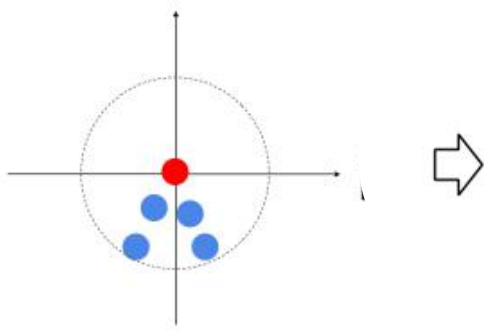
# Closer Look



# Closer Look

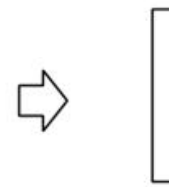


$N$  points in  $(x,y)$



$k$  local points in  $(x',y')$

*Local  
Aggregation*



# Closer Look



香港中文大學(深圳)  
The Chinese University of Hong Kong, Shenzhen



- Point-wise multi-layer perceptions (MLP) based
- Adaptive weight based
- Pseudo grid feature based

# Closer Look



香港中文大學(深圳)  
The Chinese University of Hong Kong, Shenzhen



- Point-wise multi-layer perceptions (MLP) based

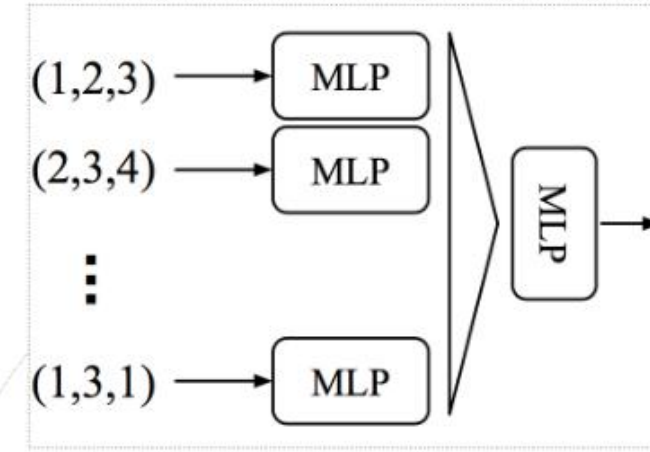
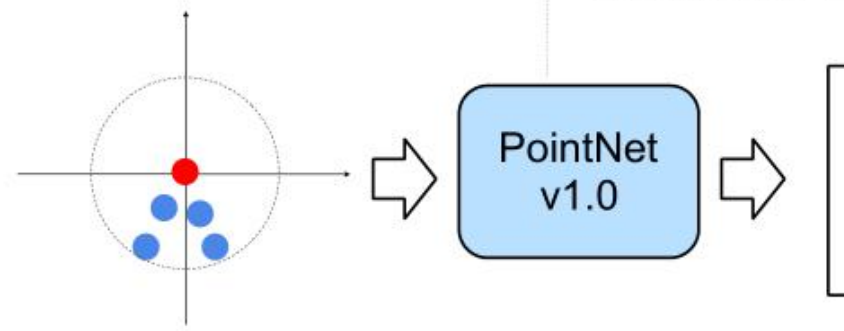
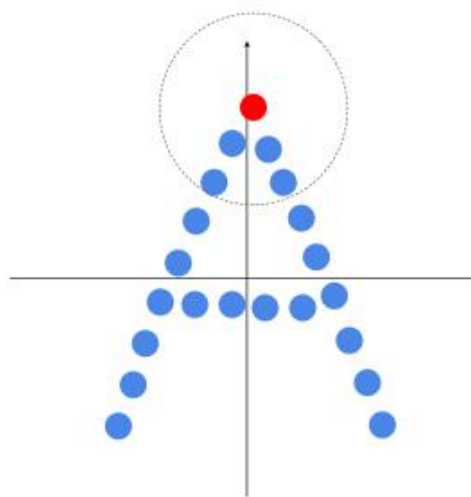
**General Formulation** In general, for each point  $i$ , a local aggregation layer first transforms a neighbor point  $j$ 's feature  $\mathbf{f}_j \in \mathbb{R}^{d \times 1}$  and its relative location  $\Delta\mathbf{p}_{ij} = \mathbf{p}_j - \mathbf{p}_i \in \mathbb{R}^{3 \times 1}$  into a new feature by a function  $G(\cdot, \cdot)$ , and then aggregate all transformed neighborhood features to form point  $i$ 's output feature by a reduction function  $R$  (typically using MAX, AVG or SUM), as

$$\mathbf{g}_i = R(\{G(\Delta\mathbf{p}_{ij}, \mathbf{f}_j) | j \in \mathcal{N}(i)\}), \quad (1)$$

where  $\mathcal{N}(i)$  represents the neighborhood of point  $i$ . Alternatively, edge features  $\{\mathbf{f}_i, \Delta\mathbf{f}_{ij}\}$  ( $\Delta\mathbf{f}_{ij} = \mathbf{f}_j - \mathbf{f}_i$ ) can be used as input instead of  $\Delta\mathbf{p}_{ij}$  [35].

$$G(\Delta\mathbf{p}_{ij}, \mathbf{f}_j) = \text{MLP}(\text{concat}(\Delta\mathbf{p}_{ij}, \mathbf{f}_j)). \quad (2)$$

# PointNet2



feature vector (mark as ■)  
for local point cloud

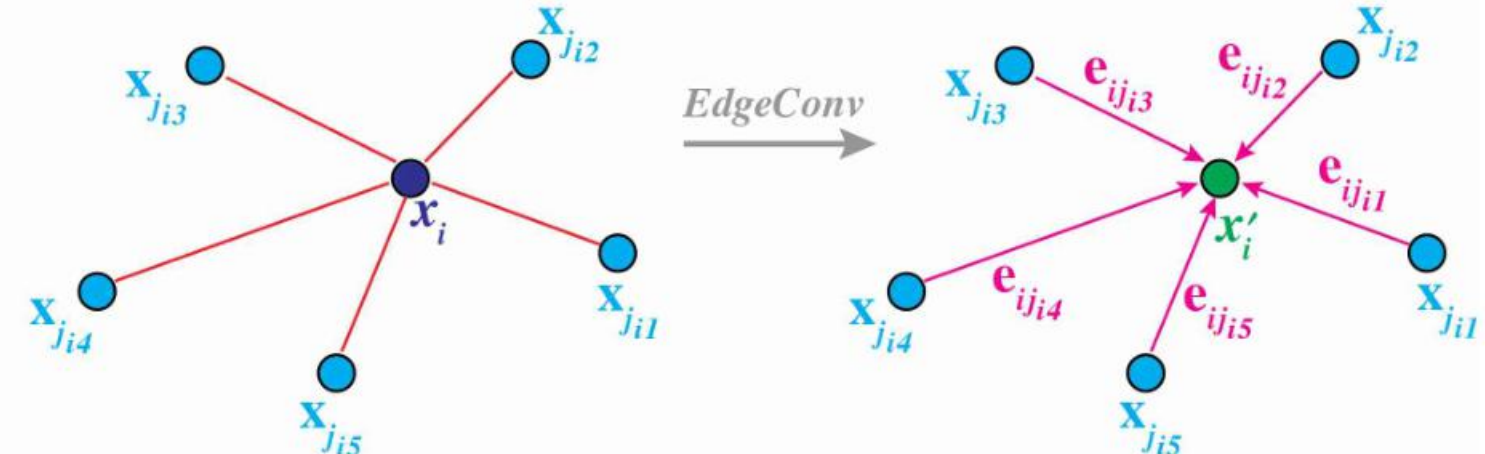
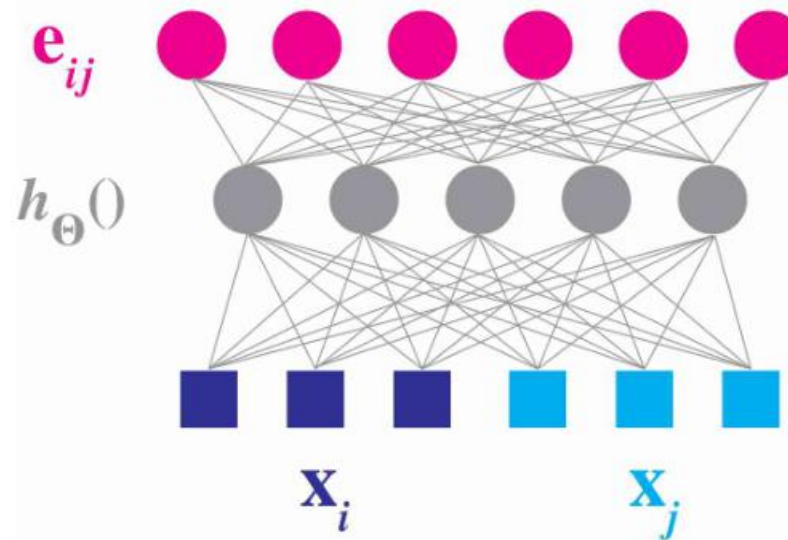
## Graph Convolution for local neighborhoods

### Dynamic Edge-Conditioned Filters in Convolutional Neural Networks on Graphs

Martin Simonovsky

Université Paris Est, École des Ponts ParisTech

[martin.simonovsky@enpc.fr](mailto:martin.simonovsky@enpc.fr)



# Closer Look



香港中文大學(深圳)  
The Chinese University of Hong Kong, Shenzhen



- Adaptive weight based

**Adaptive Weight based Methods** The adaptive weight based methods define convolution filters over arbitrary relative positions, and hence can compute aggregation weights on all neighbor points:

$$G(\Delta \mathbf{p}_{ij}, \mathbf{f}_j) = H(\Delta \mathbf{p}_{ij}) \odot \mathbf{f}_j, \quad (5)$$

## Relation-Shape Convolutional Neural Network for Point Cloud Analysis

Yongcheng Liu<sup>†‡</sup>

Bin Fan<sup>\*†</sup>

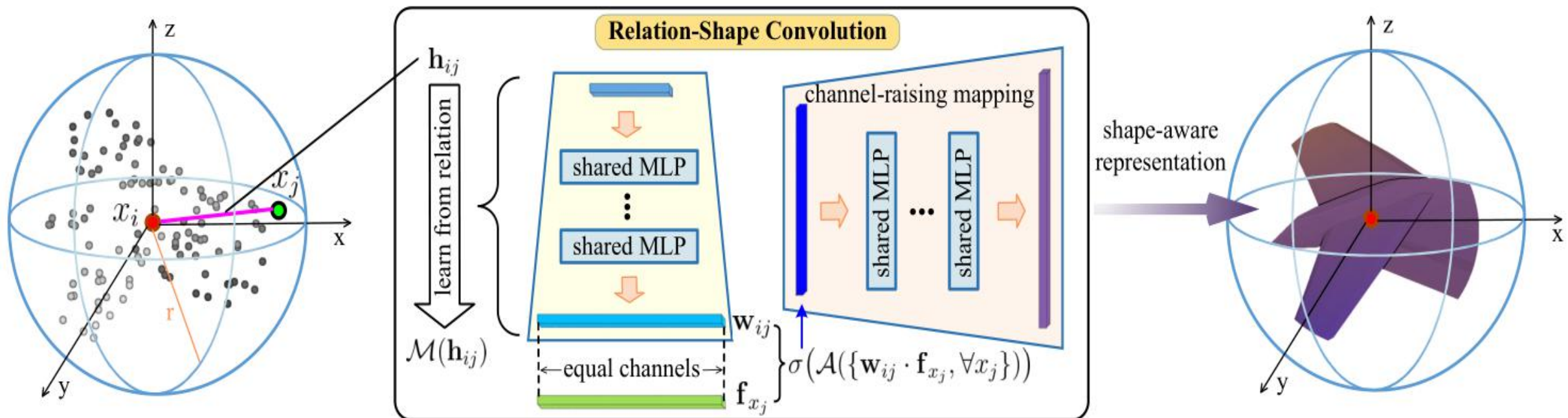
Shiming Xiang<sup>†‡</sup>

Chunhong Pan<sup>†</sup>

<sup>†</sup>National Laboratory of Pattern Recognition, Institute of Automation, Chinese Academy of Sciences

<sup>‡</sup>School of Artificial Intelligence, University of Chinese Academy of Sciences

Email: {yongcheng.liu, bfan, smxiang, chpan}@nlpr.ia.ac.cn



## Results with different relations

| model | low-level relation $\mathbf{h}$                  | channels | acc.           |
|-------|--|----------|----------------|
| A     | (3D-Ed)  | 1        | 92.5           |
| B     | (3D-Ed, $x_i - x_j$ )                            | 4        | 93.0           |
| C     | (3D-Ed, $x_i - x_j, x_i, x_j$ )                  | 10       | <b>93.6</b>    |
| D     | (3D-cosd, $x_i^{\text{nor}}, x_j^{\text{nor}}$ ) | 7        | 92.8           |
| E     | (2D-Ed, $x'_i - x'_j, x'_i, x'_j$ )              | 10       | $\approx 92.2$ |

# Closer Look



香港中文大學(深圳)  
The Chinese University of Hong Kong, Shenzhen



- Pseudo grid feature based

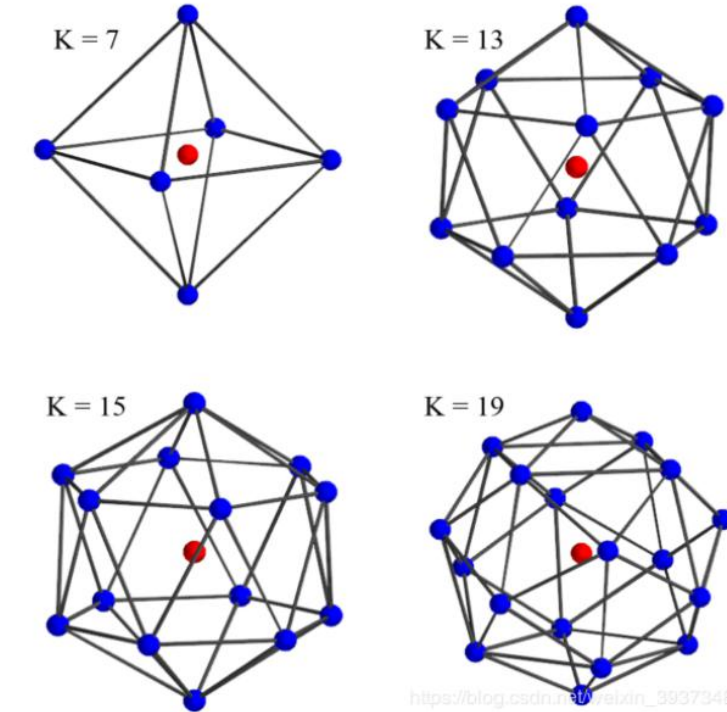
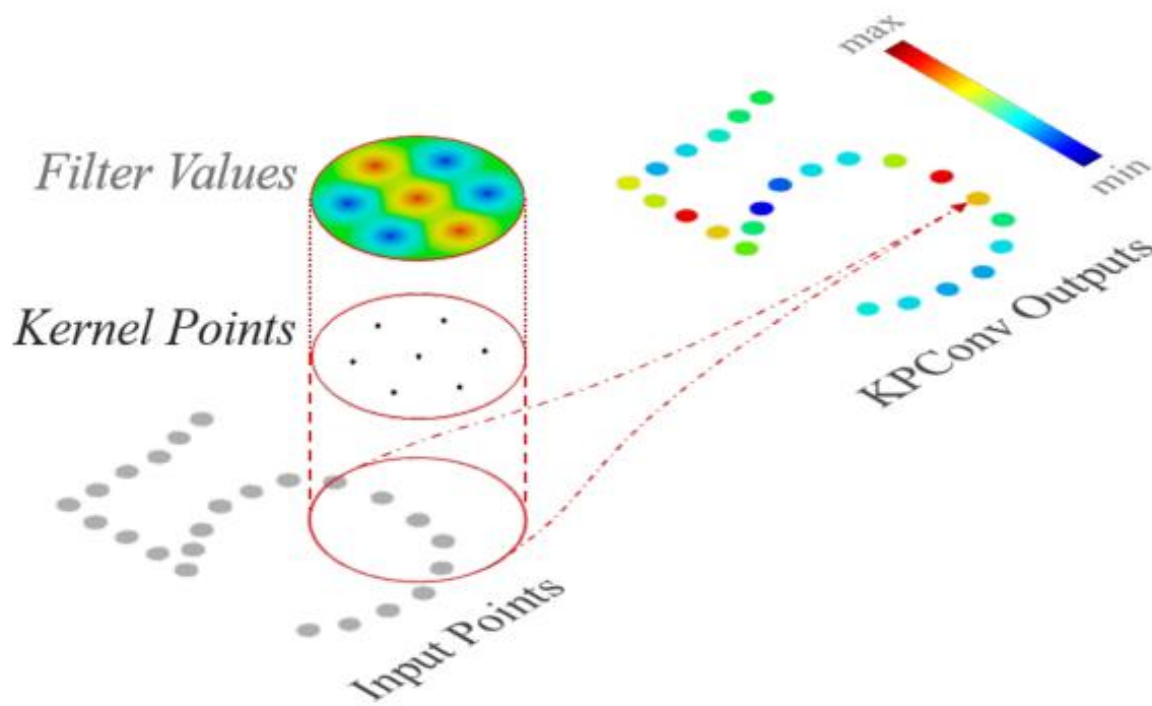
**Pseudo Grid Feature based Methods** The pseudo grid feature based methods generate pseudo features on several sampled regular grid points, such that regular convolution methods can be applied. A representative method is KP-Conv [30], where equally distributed spherical grid points are sampled and the pseudo features on the  $k^{\text{th}}$  grid point is computed as

$$\mathbf{f}_{i,k} = \sum_{j \in \mathcal{N}(i)} \max(0, 1 - \frac{\|\Delta\mathbf{p}_{jk}\|_2}{\sigma}) \cdot \mathbf{f}_j. \quad (3)$$

The index of each grid point  $k$  will have strict mapping with the relative position to center point  $\Delta\mathbf{p}_{ik}$ . Hence, a (depth-wise) convolution operator with parametrized weights  $\mathbf{w}_k \in \mathbb{R}^{d \times 1}$  defined on each grid point can be used to achieve feature transformation:

$$G(\Delta\mathbf{p}_{ik}, \mathbf{f}_{i,k}) = \mathbf{w}_k \odot \mathbf{f}_{i,k}. \quad (4)$$

# KPConv



[https://blog.csdn.net/weixin\\_39373480](https://blog.csdn.net/weixin_39373480)

# KPConv

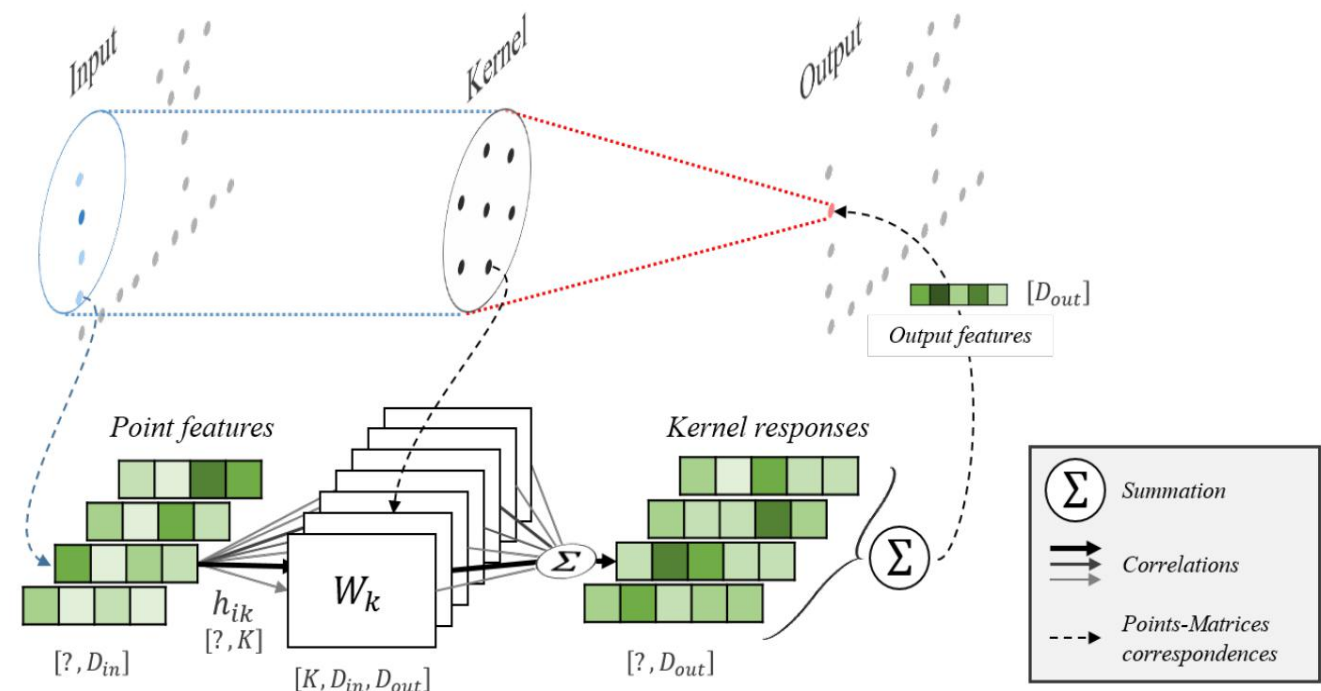
The general point convolution of  $F$  by a kernel  $g$

$$(\mathcal{F} * g)(x) = \sum_{x_i \in \mathcal{N}_x} g(x_i - x) f_i$$

Function  $g$  for KPConv

$$g(y_i) = \sum_{k < K} h(y_i, \tilde{x}_k) W_k$$

$$h(y_i, \tilde{x}_k) = \max \left( 0, 1 - \frac{\|y_i - \tilde{x}_k\|}{\sigma} \right)$$



# KPConv

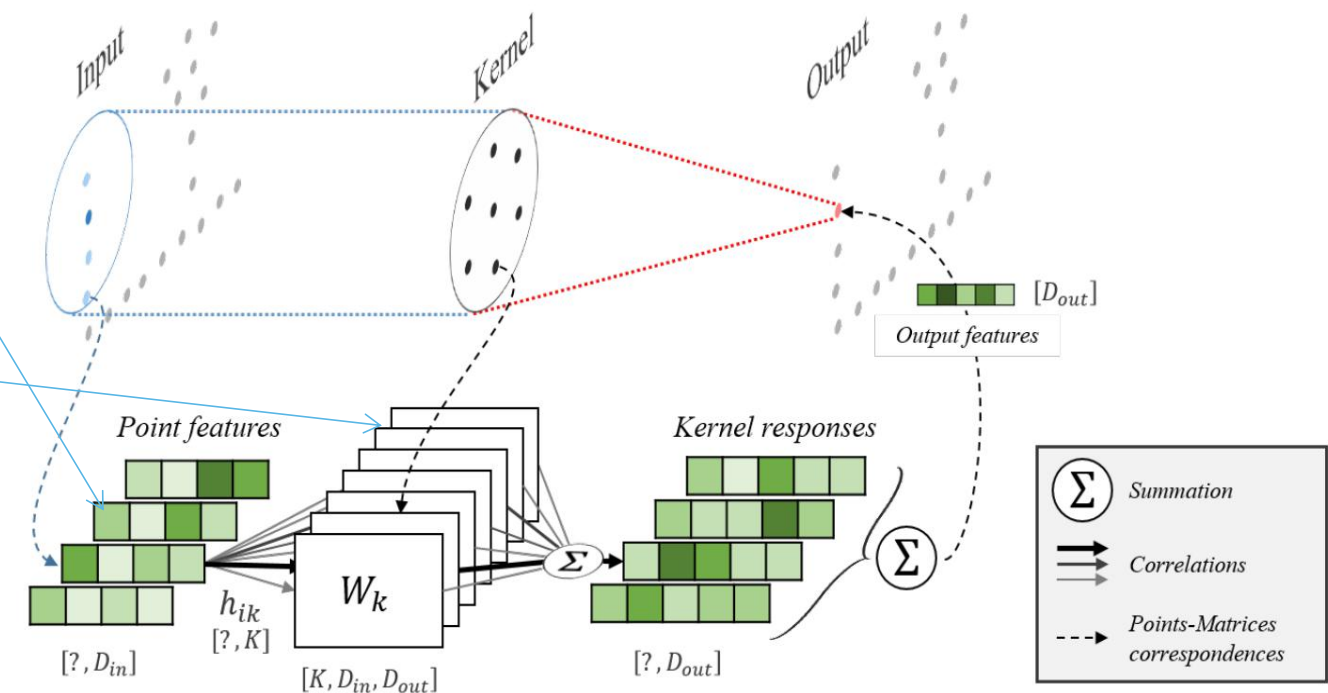
The general point convolution of  $F$  by a kernel  $g$

$$(\mathcal{F} * g)(x) = \sum_{x_i \in \mathcal{N}_x} g(x_i - x) f_i$$

Function  $g$  for KPConv

$$g(y_i) = \sum_{k < K} h(y_i, \tilde{x}_k) W_k$$

$$h(y_i, \tilde{x}_k) = \max \left( 0, 1 - \frac{\|y_i - \tilde{x}_k\|}{\sigma} \right)$$



# PosPool

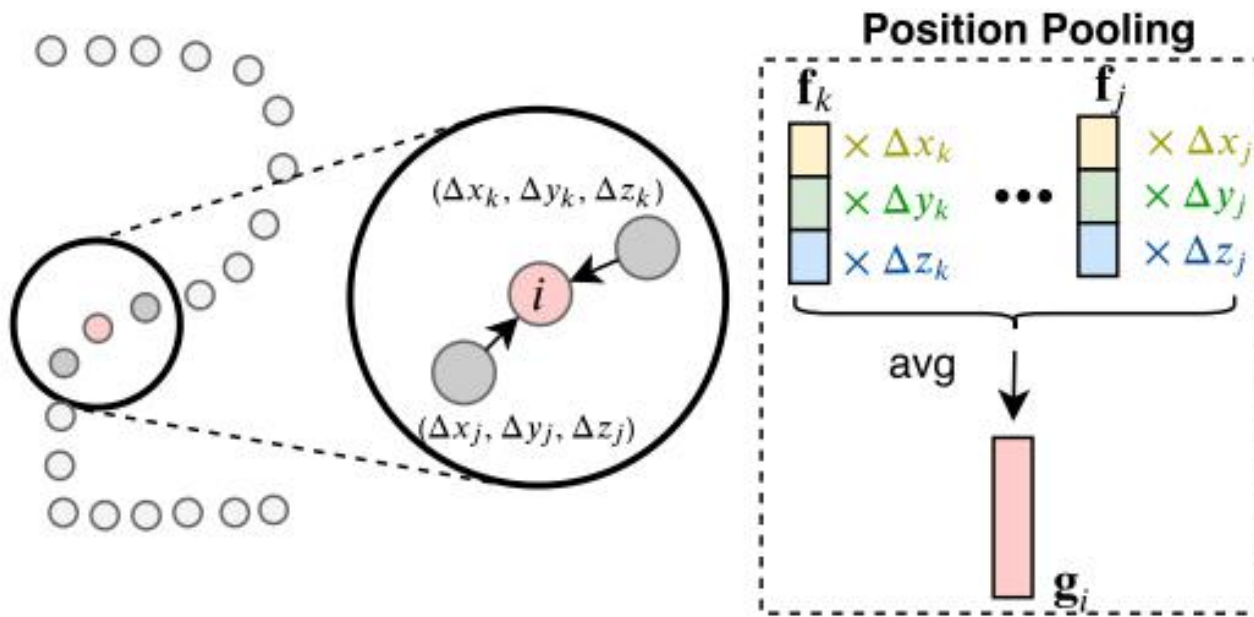


**Fig. 2.** Illustration of the proposed position pooling (PosPool) operator.

$$G(\Delta \mathbf{p}_{ij}, \mathbf{f}_j) = \text{Concat} [\Delta x_{ij} \mathbf{f}_j^0; \Delta y_{ij} \mathbf{f}_j^1; \Delta z_{ij} \mathbf{f}_j^2],$$

# Closer Look



香港中文大學(深圳)  
The Chinese University of Hong Kong, Shenzhen

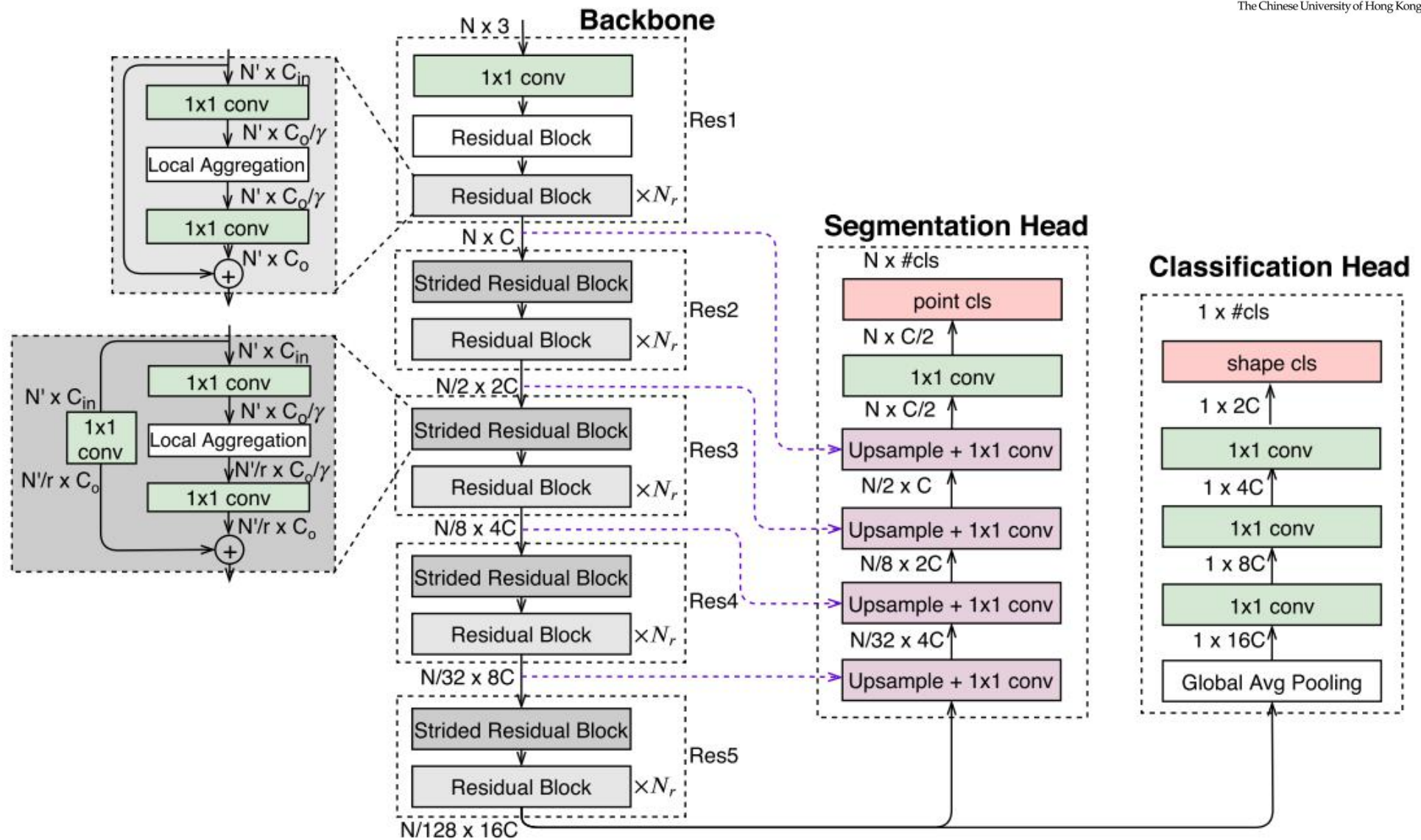


**Table 1.** The performance of baseline operators, sweet spots of point-wise MLP based, pseudo grid feature based and adaptive weight based operators, and the proposed PosPool operators on three benchmark datasets. Baseline\* denotes Eq. (6) and baseline<sup>†</sup> (AVG/MAX) denotes Eq. (7) AVG/MAX, respectively. PosPool and PosPool\* denote the operators in Eq. (8) and (10), respectively. (S) after each method denotes a smaller configuration of this method ( $N_r = 1$ ,  $\gamma = 2$  and  $C = 36$ ), which is about  $16\times$  more efficient than the regular configuration (the other row) of  $N_r = 1$ ,  $\gamma = 2$  and  $C = 144$ . Previous best performing methods on three benchmarks in literature are shown in the first block of this table

| method                         | ModelNet40 |       |       | S3DIS |       |       | PartNet |      |       |       |
|--------------------------------|------------|-------|-------|-------|-------|-------|---------|------|-------|-------|
|                                | acc        | param | FLOP  | mIoU  | param | FLOP  | val     | test | param | FLOP  |
| DensePoint [15]                | 93.2       | 0.7M  | 0.7G  | -     | -     | -     | -       | -    | -     | -     |
| KPConv [30]                    | 92.9       | 15.2M | 1.7G  | 65.7  | 15.0M | 6.5G  | -       | -    | -     | -     |
| PointCNN [14]                  | 92.5       | 0.6M  | 25.3G | 65.4  | 4.4M  | 36.7G | -       | 46.4 | 4.4M  | 23.1G |
| baseline*                      | 91.4       | 19.4M | 1.8G  | 51.5  | 18.4M | 7.2G  | 42.5    | 44.6 | 18.5M | 6.7G  |
| baseline <sup>†</sup> (AVG, S) | 90.7       | 1.2M  | 0.1G  | 50.3  | 1.1M  | 0.5G  | 39.5    | 40.6 | 1.1M  | 0.4G  |
| baseline <sup>†</sup> (AVG)    | 91.4       | 19.4M | 1.8G  | 51.0  | 18.4M | 7.2G  | 44.2    | 45.8 | 18.5M | 6.7G  |
| baseline <sup>†</sup> (MAX, S) | 91.5       | 1.2M  | 0.1G  | 57.4  | 1.1M  | 0.5G  | 39.8    | 41.2 | 1.1M  | 0.4G  |
| baseline <sup>†</sup> (MAX)    | 91.8       | 19.4M | 1.8G  | 58.4  | 18.4M | 7.2G  | 45.4    | 47.4 | 18.5M | 6.7G  |
| point-wise MLP (S)             | 92.6       | 1.7M  | 0.2G  | 56.7  | 1.6M  | 0.8G  | 45.3    | 47.0 | 1.6M  | 0.7G  |
| point-wise MLP                 | 92.8       | 26.5M | 2.7G  | 66.2  | 25.5M | 9.8G  | 48.1    | 51.5 | 25.6M | 9.1G  |
| pseudo grid (S)                | 92.3       | 1.2M  | 0.3G  | 64.3  | 1.2M  | 1.0G  | 44.2    | 45.2 | 1.2M  | 0.9G  |
| pseudo grid                    | 93.0       | 19.5M | 2.0G  | 65.9  | 18.5M | 9.3G  | 50.8    | 53.0 | 18.5M | 8.5G  |
| adapt weights (S)              | 92.1       | 1.2M  | 0.2G  | 61.9  | 1.2M  | 0.6G  | 44.1    | 46.1 | 1.2M  | 0.5G  |
| adapt weights                  | 93.0       | 19.4M | 2.3G  | 66.5  | 18.4M | 7.8G  | 50.1    | 53.5 | 18.5M | 7.2G  |
| PosPool (S)                    | 92.5       | 1.2M  | 0.1G  | 64.2  | 1.1M  | 0.5G  | 44.6    | 47.2 | 1.1M  | 0.5G  |
| PosPool                        | 92.9       | 19.4M | 1.8G  | 66.5  | 18.4M | 7.3G  | 50.0    | 53.4 | 18.5M | 6.8G  |
| PosPool* (S)                   | 92.6       | 1.2M  | 0.1G  | 61.3  | 1.1M  | 0.5G  | 46.1    | 47.2 | 1.1M  | 0.5G  |
| PosPool*                       | 93.2       | 19.4M | 1.8G  | 66.7  | 18.4M | 7.3G  | 50.6    | 53.8 | 18.5M | 6.8G  |

**Table 2.** Evaluating different settings of the point-wise MLP method. The option  $\nabla$ ,  $\Delta$ ,  $\square$  and  $\diamond$  denote input features using  $\{\Delta\mathbf{p}_{ij}, \mathbf{f}_j\}$ ,  $\{\mathbf{f}_i, \Delta\mathbf{f}_{ij}\}$ ,  $\{\Delta\mathbf{p}_{ij}, \mathbf{f}_i, \Delta\mathbf{f}_{ij}\}$ , and  $\{\Delta\mathbf{p}_{ij}, \mathbf{f}_i, \mathbf{f}_j, \Delta\mathbf{f}_{ij}\}$ , respectively. “Sweet spot” denotes balanced settings regarding both efficacy and efficiency. The accuracy on PartNet test set is not tested in ablations to avoid the tuning of test set

| method               | $\gamma$ | input    |          | #FC | $R(\cdot)$ | ModelNet40 | S3DIS | PartNet<br>(val/test) |
|----------------------|----------|----------|----------|-----|------------|------------|-------|-----------------------|
|                      |          | $\nabla$ | $\Delta$ |     |            |            |       |                       |
| PointNet++ [22]      | -        | ✓        |          | 3   | MAX        | 90.7       | -     | -/42.5                |
| PointNet++*          | -        | ✓        |          | 3   | MAX        | 91.6       | 55.3  | 43.1/45.3             |
| sweet spot           | 8        | ✓        |          | 1   | MAX        | 92.8       | 62.9  | 48.2/50.8             |
|                      | 2        | ✓        |          | 1   | MAX        | 92.8       | 66.2  | 48.1/51.2             |
| FC num               | 8        | ✓        |          | 2   | MAX        | 92.5       | 59.5  | 47.9/-                |
|                      | 8        | ✓        |          | 3   | MAX        | 92.0       | 59.9  | 48.7/-                |
| input                | 8        | ✓        |          | 1   | MAX        | 92.6       | 59.8  | 47.1/-                |
|                      | 8        | ✓        |          | 1   | MAX        | 92.5       | 61.4  | 47.6/-                |
|                      | 8        |          | ✓        | 1   | MAX        | 92.7       | 51.0  | 47.9/-                |
| reduction $R(\cdot)$ | 8        | ✓        |          | 1   | AVG        | 92.3       | 55.1  | 46.8/-                |
|                      | 8        | ✓        |          | 1   | SUM        | 92.2       | 44.7  | 46.7/-                |

**Sweet spots for point-wise MLP methods.** Regarding both the efficacy and efficiency, the sweet spot settings are applying 1 FC layer to an input combination of relative position and edge features. Table 2 also shows that using  $\gamma = 2$  for this method can approach or surpass the state-of-the-art on all three datasets.

**Table 3.** Evaluating different settings of the adaptive weight based methods.  $dp^*$  denotes the 9-dimensional position vector as in [16]. “Sweet spot” denotes balanced settings regarding both efficacy and efficiency. The accuracy on PartNet test set is not tested for ablations to avoid tuning the test set.

| method      | $\gamma$ | input    |          | #FC | $R(\cdot)$ | S.M. | ModelNet | S3DIS | PartNet<br>(val) |
|-------------|----------|----------|----------|-----|------------|------|----------|-------|------------------|
|             |          | $\{dp\}$ | $\{df\}$ |     |            |      |          |       |                  |
| PConv[34]   | -        | ✓        |          | 2   | SUM        |      | -        | 58.3  | -                |
| FlexConv[5] | -        | ✓        |          | 1   | SUM        |      | 90.2     | 56.6  | -                |
| sweet spot  | 8        | ✓        |          | 1   | AVG        |      | 92.7     | 62.6  | 50.0             |
| sweet spot* | 2        | ✓        |          | 1   | AVG        |      | 93.0     | 66.5  | 50.1             |
| FC num      | 8        | ✓        |          | 2   | AVG        |      | 92.6     | 61.3  | 49.9             |
|             | 8        | ✓        |          | 3   | AVG        |      | 92.5     | 58.5  | 49.6             |
| input       | 8        |          | ✓        | 1   | AVG        |      | 85.3     | 46.6  | 46.9             |
|             | 8        |          | ✓        | 1   | AVG        |      | 82.2     | 55.7  | 46.4             |
|             | 8        |          |          | ✓   | AVG        |      | 92.1     | 57.0  | 49.1             |
| reduction   | 8        | ✓        |          | 1   | SUM        |      | 92.6     | 61.7  | 49.1             |
|             | 8        | ✓        |          | 1   | MAX        |      | 92.4     | 62.3  | 49.7             |
| SoftMax     | 8        | ✓        |          | 1   | AVG        | ✓    | 91.7     | 55.9  | 45.8             |

**Sweet spots for adaptive weight based methods.** The best performance is achieved by applying 1 FC layer without SoftMax normalization on relative positions alone to compute the adaptive weights. This method also approaches or surpasses the state-of-the-art on all three datasets using a deep residual network.



# *Towards Content-Independent Multi-Reference Super-Resolution: Adaptive Pattern Matching and Feature Aggregation*

*Xu Yan<sup>\*</sup> <sub>1</sub>, Weibing Zhao<sup>\*</sup> <sub>1</sub>, Kun Yuan <sub>1,2</sub>, Ruimao Zhang <sub>3</sub>,  
Zhen Li<sup>†</sup> <sub>1</sub> and Shuguang Cui <sub>1</sub>*

<sub>1</sub> The Chinese University of Hong Kong (Shenzhen),  
Shenzhen Research Institute of Big Data,

<sub>2</sub> University of Ottawa, <sub>3</sub> SenseTime Research

# Single image super-resolution

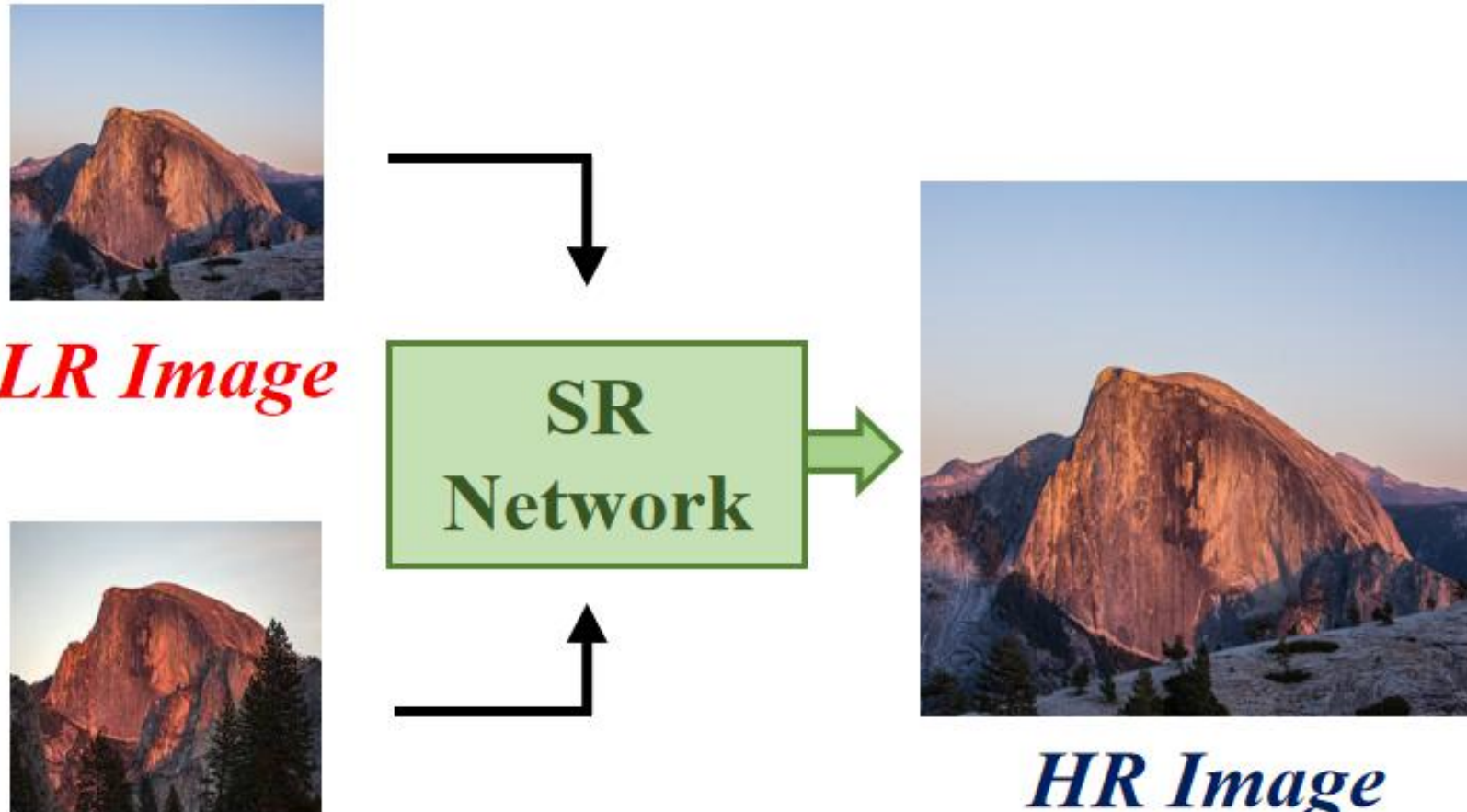


*LR Image*



*HR Image*

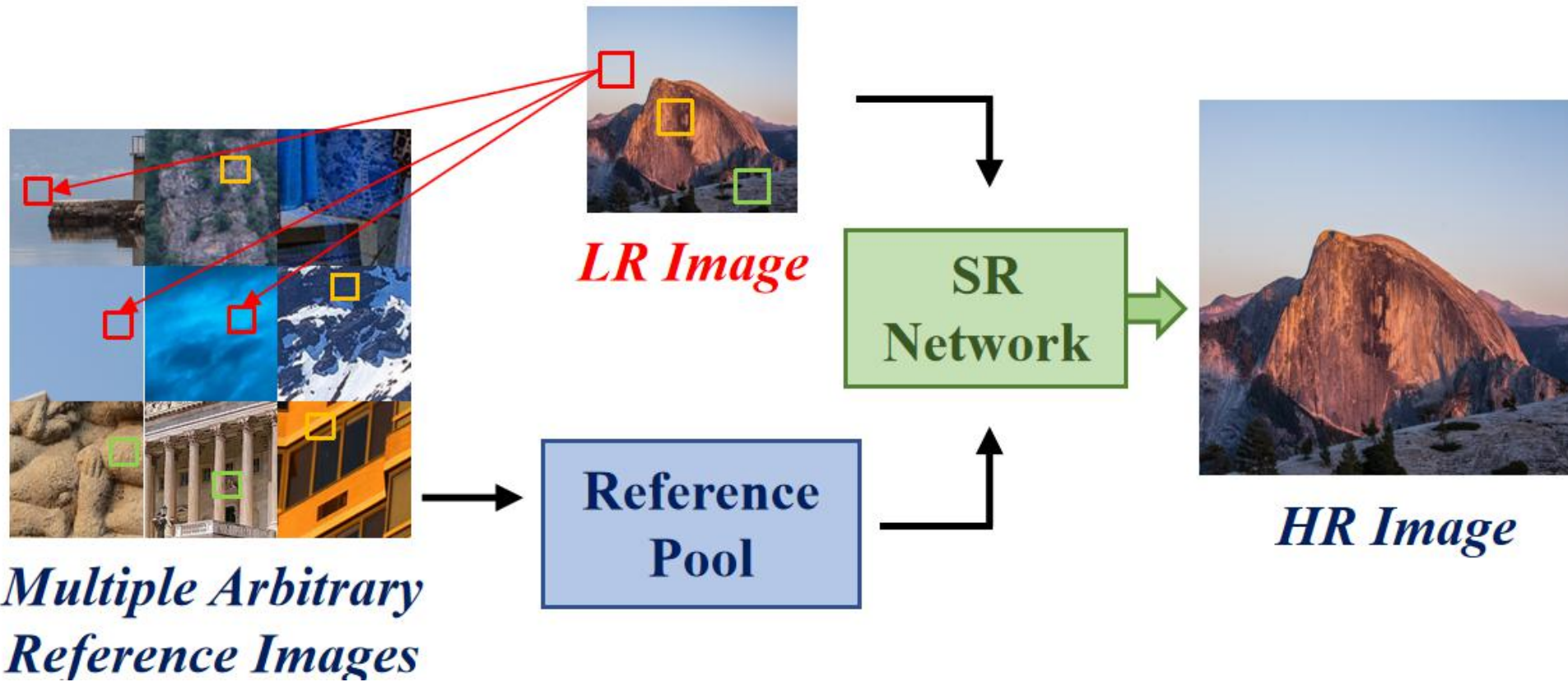
# Reference-based super-resolution



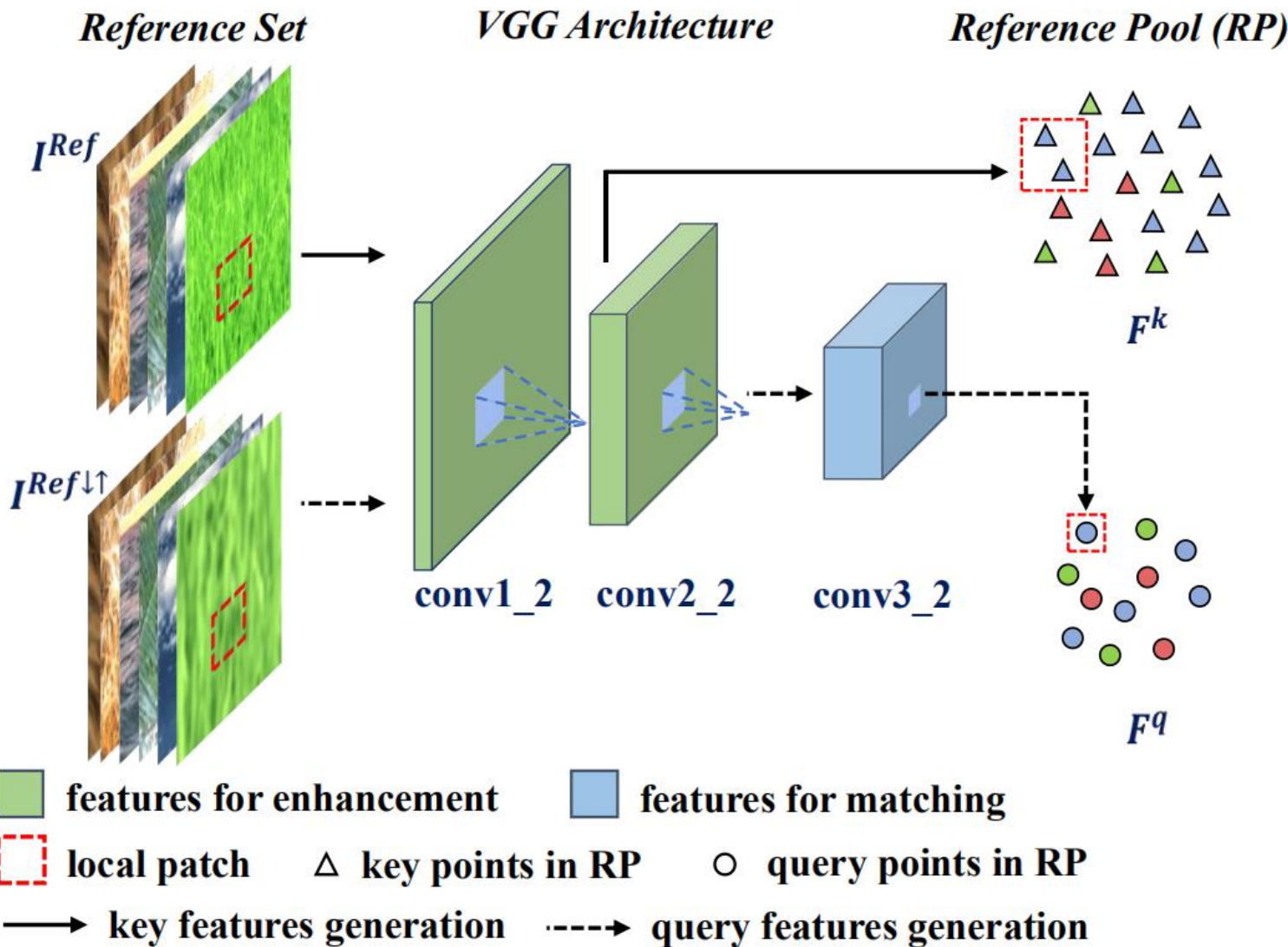
*Single Similar Reference Image*

# CIMR-SR

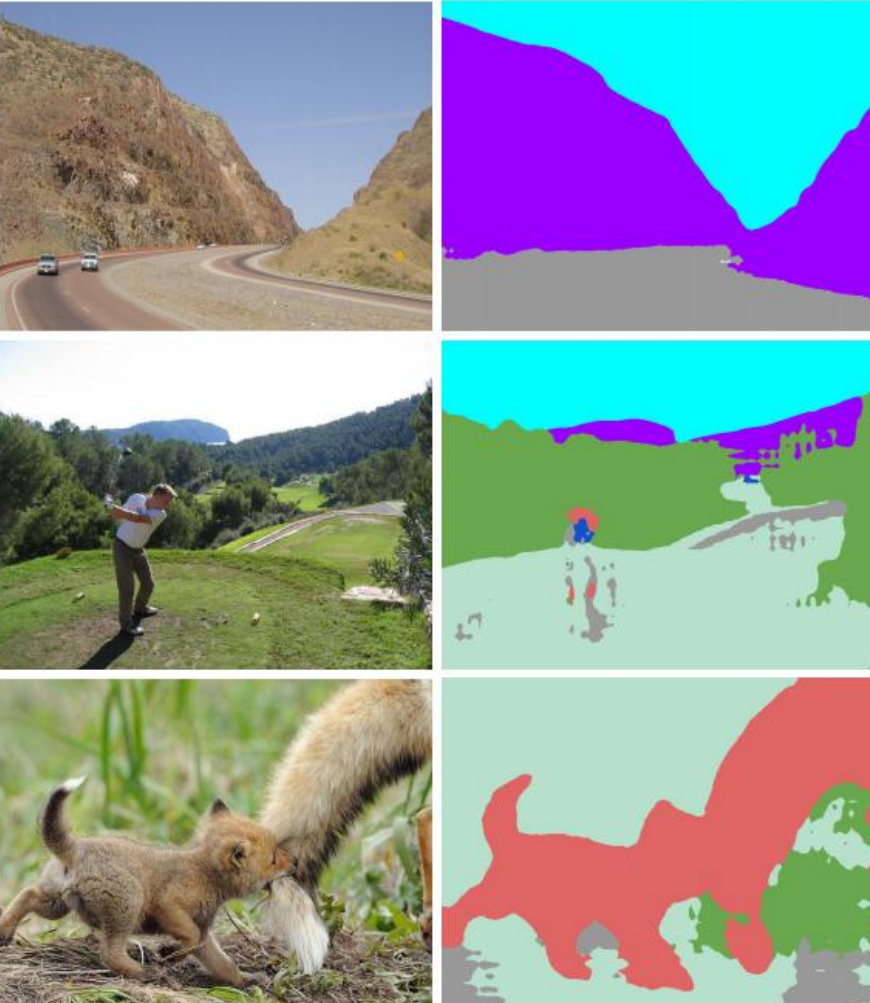
Content-independent multi-reference super-resolution



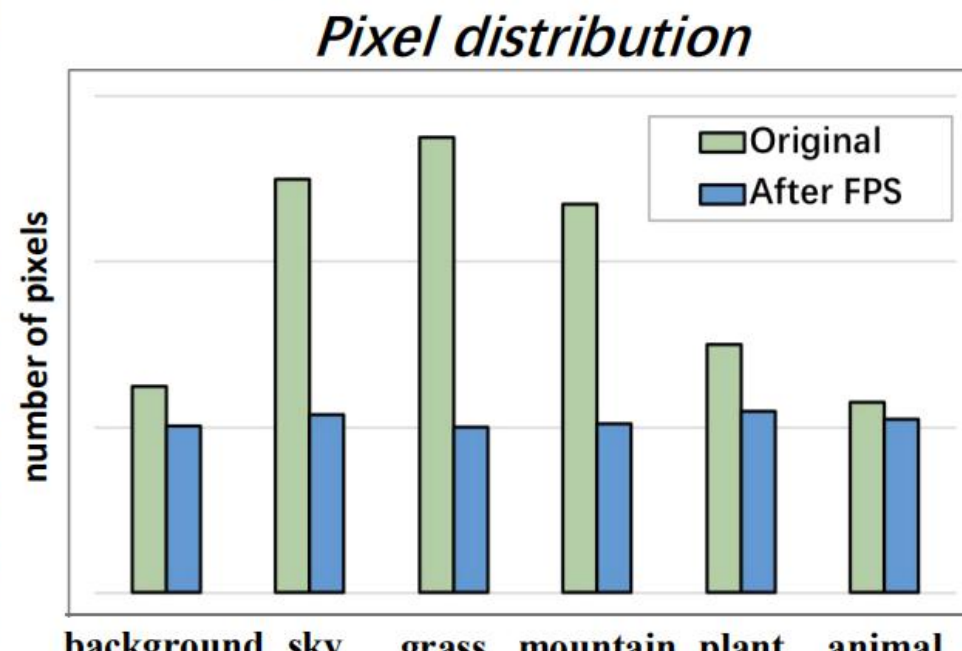
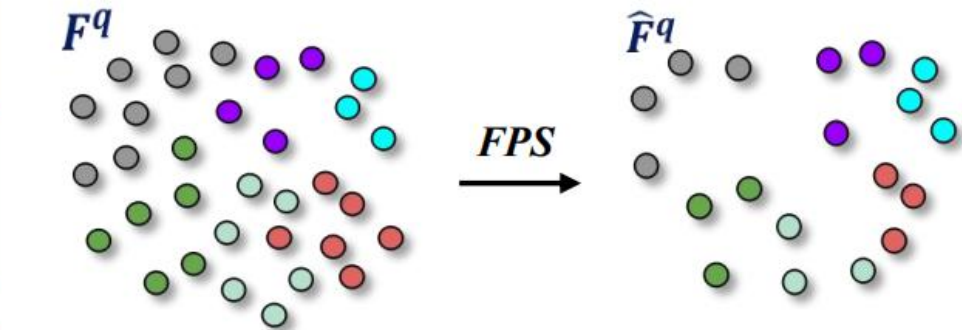
# CIMR to feature space



# Farthest Point Sampling (FPS)

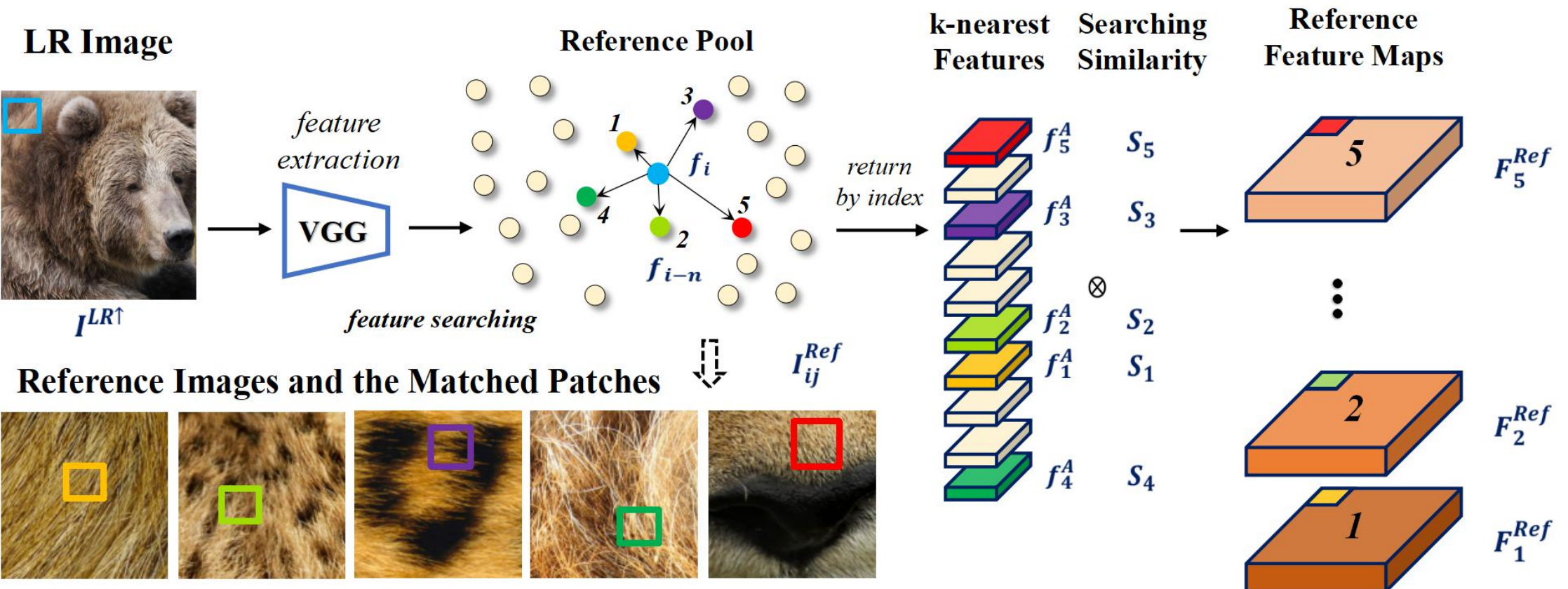


■ sky ■ mountain ■ background ■ plant ■ grass ■ animal ■ building

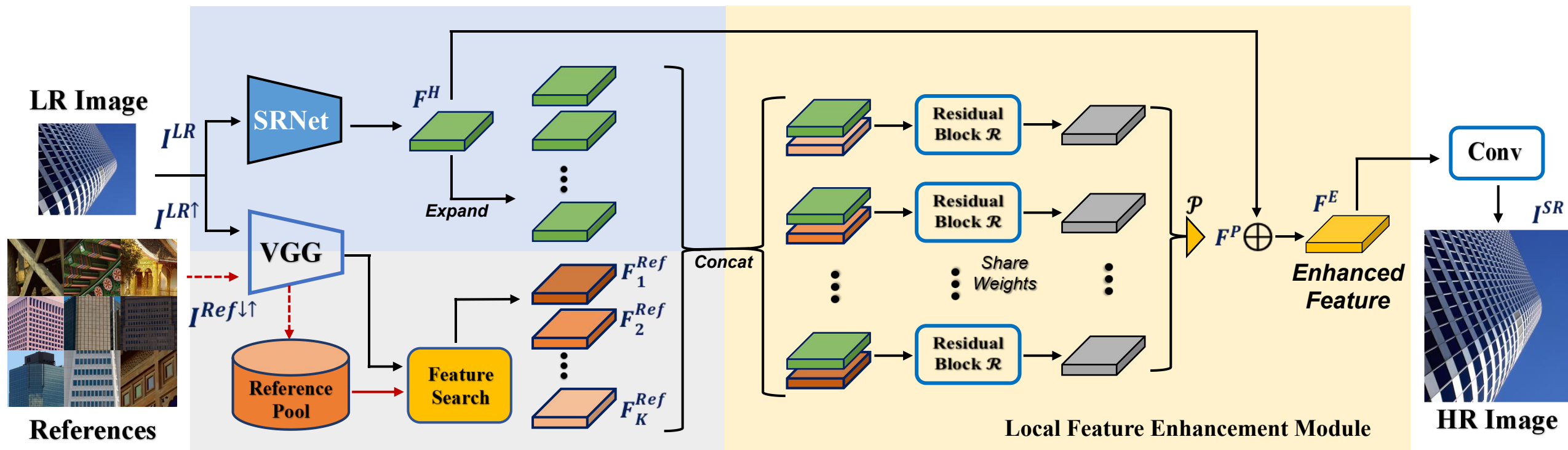


- **Feature Searching** retrieves K most similar feature points from query features for each local patch of input LR
- **Feature Aggregation** aligns and fuses the searched key features and generates enhanced feature maps for HR reconstruction

# Feature searching



# Feature aggregation



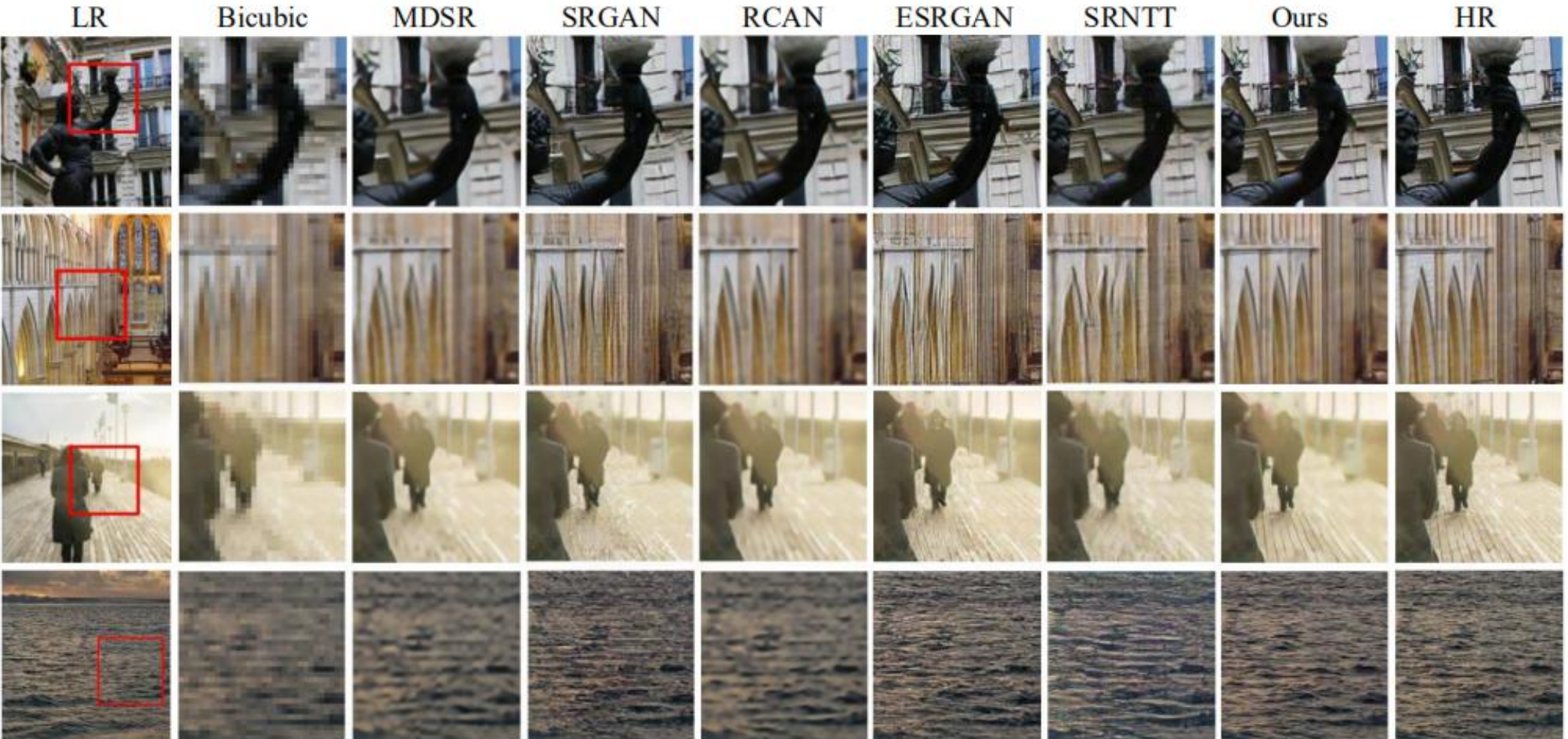
# Results

**Table 1.** PSNR/SSIM comparison among different SR methods on four datasets: methods are grouped by SISR (top) and RefSR (bottom), and the best result is in bold. All the SR results are evaluated by PSNR and SSIM metrics on the Y channel of transformed YCbCr space.

| Algorithm             | CUFED5               | Urban100             | Sun80                |
|-----------------------|----------------------|----------------------|----------------------|
| Bicubic               | 24.18 / 0.684        | 23.14 / 0.674        | 27.24 / 0.739        |
| SRCNN [4]             | 25.33 / 0.745        | 24.41 / 0.738        | 28.26 / 0.781        |
| SCN [26]              | 25.45 / 0.743        | 24.52 / 0.741        | 27.93 / 0.786        |
| DRCN [12]             | 25.26 / 0.734        | 25.14 / 0.760        | 27.84 / 0.785        |
| LapSRN [13]           | 24.92 / 0.730        | 24.26 / 0.735        | 27.70 / 0.783        |
| MDSR [15]             | 25.93 / 0.777        | 25.51 / 0.783        | 28.52 / 0.792        |
| EDSR [15]             | 25.90 / 0.776        | 25.50 / 0.783        | 28.49 / 0.789        |
| SRGAN [14]            | 24.40 / 0.702        | 24.07 / 0.729        | 26.76 / 0.725        |
| RCAN [33]             | <b>26.32 / 0.789</b> | <b>25.65 / 0.785</b> | <b>28.67 / 0.795</b> |
| SAN [3]               | 26.29 / 0.789        | 25.63 / 0.783        | 28.66 / 0.795        |
| LandMark [30]         | 24.91 / 0.718        | -                    | 27.68 / 0.776        |
| CrossNet [36]         | 25.48 / 0.764        | 25.11 / 0.764        | 28.52 / 0.793        |
| SRNTT [35]            | 25.61 / 0.764        | 25.09 / 0.774        | 27.59 / 0.756        |
| CIMR                  | 26.16 / 0.781        | 25.24 / 0.778        | 29.67 / 0.806        |
| SRNTT $^*\ell_2$ [35] | 25.98 / 0.776        | 25.54 / 0.784        | 28.49 / 0.791        |
| SRNTT- $\ell_2$ [35]  | 26.24 / 0.784        | 25.50 / 0.783        | 28.54 / 0.793        |
| CIMR- $\ell_2$        | <b>26.35 / 0.789</b> | <b>25.77 / 0.792</b> | <b>30.07 / 0.813</b> |

## Content-independent references

# Results



# Results

## Content-similar references

**Table 2.** PSNR/SSIM at different reference levels on CUFED5 dataset. The "warp" denotes the data augmentation with random translation (quarter to half width/height), rotation (10~30 degree), and scaling (1.2~2.0× upscaling) from the original HR image.

| Algorithm       | HR (warp)         | L1                | L2                | L3                | L4                | All               |
|-----------------|-------------------|-------------------|-------------------|-------------------|-------------------|-------------------|
| CrossNet        | 25.49/.764        | 25.48/.764        | 25.48/.764        | 25.47/.763        | 25.46/.763        | -                 |
| SRNTT- $\ell_2$ | 29.29/.889        | 26.15/.781        | 26.04/.776        | 25.98/.775        | 25.95/.774        | 26.24/.784        |
| CIMR- $\ell_2$  | 29.82/.903        | <b>27.32/.805</b> | <b>27.05/.799</b> | <b>26.92/.796</b> | <b>26.86/.794</b> | <b>27.44/.810</b> |
| SRNTT           | <b>33.87/.959</b> | 25.42/.758        | 25.32/.752        | 25.24/.751        | 25.23/.750        | 25.61/.764        |
| CIMR            | 30.73/.918        | 26.50/.786        | 26.47/.784        | 26.45/.784        | 26.44/.784        | 26.63/.790        |



# Results

**Table 3.** Comparison of adopting different conv layers for CIMR. Left part shows PSNR at different reference levels on CUFED5 test set. Right part describes running time, including offline feature searching and forward inference time.

| Method- $\ell_2$ | HR(warp)     | L1           | L2           | L3           | L4           | FS           | Forward      |
|------------------|--------------|--------------|--------------|--------------|--------------|--------------|--------------|
| SRNTT            | 29.29        | 26.15        | 26.04        | 25.98        | 25.95        | 2.726        | <b>0.351</b> |
| conv1            | 28.24        | 26.97        | 26.89        | 26.84        | 26.79        | 2.045        | 0.783        |
| conv2            | 28.77        | 27.06        | 26.93        | 26.92        | 26.85        | 1.551        | 0.535        |
| conv3            | 27.31        | 26.26        | 26.06        | 26.02        | 26.03        | <b>1.020</b> | 0.361        |
| conv2/3          | 27.87        | 27.27        | 27.01        | 26.89        | 26.82        | 2.571        | 1.077        |
| conv1/2/3        | <b>29.82</b> | <b>27.32</b> | <b>27.05</b> | <b>26.92</b> | <b>26.86</b> | 4.616        | 1.551        |



香港中文大學(深圳)  
The Chinese University of Hong Kong, Shenzhen



*Thanks for watching!*

Xu Yan  
2020.8.20